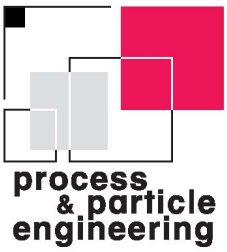

Measurement of Rheology and Adhesion of Pharmaceutical Hot Melt Extrusion Matrix Carriers

Clemens-Michael Smola

Institute of Particle and Process Engineering &

Research Center Pharmaceutical Engineering

University of Technology, Graz

Advisor

Prof. Johannes Khinast

Supervisor

Daniel Treffer

Acknowledgements

First of all I would like to thank Daniel Treffer for giving me a great introduction into the subject and guiding me through the whole experimental and theoretical background of this work.

Furthermore, I would like to thank Sarah Windhab for instructing me on working with the Rheometer and Prof. Andreas Zimmer from the Institute of Pharmaceutical Technology of Karl-Franzens University for being so kind to grant me access to their facilities. In addition I would like to thank the whole team form the Research center for Pharmaceutical Engineering, who made my time just the more enjoyable; including Gerold Koscher, Simone Schrank and Andreas Eitzlmayr.

Last but by no means least I would like to thank Professor Johannes Khinast for being my thesis advisor and giving me the great opportunity of becoming a well integrated member of his team and being able to produce such sound work together with inspiring colleagues and friends.

Declaration

The work presented in this diploma thesis is to my best of knowledge and believe, original, except as acknowledged in the text. This material has not been submitted, either in the whole or in part, for a degree at this or any other university.

_____ _____

Place, Date Signature

Eidesstattliche Erklärung

Ich erkläre an Eides Statt, dass ich die vorliegende Arbeit selbstständig und ohne fremde Hilfe verfasst, andere als die angegebenen Quellen nicht benutzt und die den benutzten Quellen wörtlich und inhaltlich entnommenen Stellen als solche kenntlich gemacht habe. Ich versichere, dass ich dieses Diplomarbeitsthema bisher weder im In- noch im Ausland in irgendeiner Form als Prüfungsarbeit vorgelegt habe.

_____ _____

Ort, Datum Unterschrift

INDEX

List of Figures and Tables

Abstract

Hot Melt Extrusion (HME) is indisputably the most important procedure in the polymer processing industry. Only recently have pharmaceutical researchers introduced the viable HME process as a novel approach to improve bioavailability, controlled release and drug efficacy and safety. The process design principles require a fundamental understanding of the handled material's Rheology.

In this work we present the basic principles of Rheology and polymer adhesion are discussed and its history explored. Multiple test stands and assays are compared and literature background, if available used to ratify innovative theories. Two substances; one polymer, Soluplus®, and one steric acid, calcium stearate, were investigated in the experimental part. Soluplus® is widely used in HME process, while calcium stearate has only been recently suggested by E. Roblegg [*]. Otherwise, hardly any long-established literature can be found in this area, which is seen as highly motivating in creating property profiles for pharmaceutical polymers.

Both substances have been rheologically analyzed by Amplitude, Temperature and Frequency tests to characterize their Rheology and subsequently create a basic understanding in regard for testing their adhesiveness. An MCR 301 Anton Paar Rheometer was used in all experimental procedures.

The presented basic oscillatory measurements of pharmaceutical Polymers to characterize and identify the substances' fundamental properties show good reproducibility and agreement with literature data as available, due to the uniform sample preparation especially developed for these experiments. It is consequently used to create better dimensioning for the HME process. As for the adhesion measurements, data recorded was contradictive and further research has to be conducted in this area.

References:

[*] Roblegg E., Jaeger E., Hodzic A., Koscher G., Mohr S., Zimmer A., Khinast J.; Development of sustained release lipophilic calcium stearate pellets via hot melt extrusion; European journal of pharmaceutics and Biopharmaceutic, Vol.79, 635-645, (2011)

CHAPTER I

1.1 Hot-Melt Extrusion

Pharmaceutical scientists consider rheology as a platform to gain insight on Hot Melt Extrusion process. The process dimensions and parameters predicate on viscosity and viscoelastic characteristics of the formulation. Paramount for our motivation to conduct such research was that there had been very little previous studies on the subject concerning pharmaceutical ingredients, which is reflected in the fact that there are hardly any literature references available to date.

It has been estimated that 40–60% of drugs in development have poor bioavailability due to low aqueous solubility. This percentage is likely to increase in the future with the increased use of combinatorial chemistry in drug discovery targeting lipophilic receptors. Poor bioavailability results in increased development times, decreased efficacy, increased inter- and intra-patient variability and side effects, and higher dosages that reduce patient compliance and increase cost [1].

Thus, the ability to improve drug solubility and hence bioavailability through formulation and process technology is critical to improving a drug product's efficacy and safety and reducing its cost. HME is the process of applying heat and pressure to melt a polymer and force it through an orifice in a continuous process [2]. By HME it is possible to improve bioavailability of ''difficult'' actives by the formation of solid dispersions and solid solutions. This is relevant for poorly soluble pharmaceutically active substances, frequently encountered among novel active ingredients [2]. Hot Melt extrusion is of particular interest for dispersing APIs in a matrix at the molecular level, thus forming solid solutions. As the drug development branch is constantly noting an increase in poorly soluble chemical entities, the technique is currently becoming more important then ever [5].

Furthermore, the formation of solid dispersion offers great possibilities for the manufacturing of controlled release formulations and dosage forms.

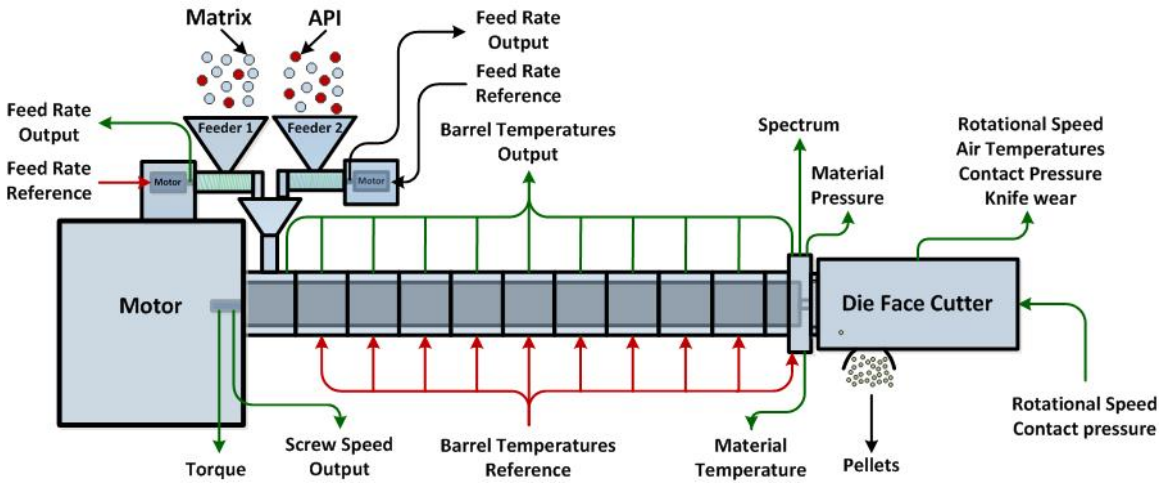

Figure 1: Schematic illustration of an extruder set up [3]

Various pharmaceutical applications perform with low soluble APIs, thus the call for improving the solubility of the compounds was large. Recently, a number of research groups have demonstrated Hot-Melt Extrusion processes as being viable techniques for the preparation of pharmaceutical drug delivery systems. Accordingly, various dosage forms can be manufactured by HME, including pellets, granules, sustainable release tablets and transdermal drug delivery systems. Unlike other pharmaceutical production processes, hot-melt extrusion has the advantage of being a solvent free, cost-efficient and most importantly, environmental friendly technology [4].

1.2 An Introduction to Rheology

1.2.1 What is Rheology

The meaning Rheology originates from the Greek word 'rheos', which is translated to River, Flow or Stream. In scientific terms, rheology is seen as the science of deformation and flow of matter under controlled testing conditions and is applicable to all types of materials, from gases to solids. Looking back, the science of rheology is very young, only about 80 years ago the American Society of Rheology was found on 29th of April 1929. On the contrary, its history nevertheless, is very old. Professor M. Reiner derived and translated the prophetess Deborah's term: "The mountains flowed before the Lord….", into a rheological expression, meaning; "*everything flows, if you wait long enough….*" It was also described by the Greek philosopher Heraclitus as "panta rei"- *everything flows.* Reiner together with E. Bingham was the founder of the science of rheology in the mid-20's, but of course the first mathematical fundamentals were derived by Sir Isaac Newton [6].

1.2.2 Two Plate Model

The simplest model to illustrate rheological properties is the Two-Plate model or also referred to as the parallel-plate model. In this test stand the top plate, which has a contact area A [m^2], is moved by normal force F [N] at a speed v [m/s], while the bottom plate remains at rest. The gap between plates is filled with fluid and the distance between the plates is described by h [m]. The boundary between the fluid and plate follows the 'no slip' condition, where the fluid moves juxtapose to the boundary with the same velocity as the plate. Consequently, the thinnest layers of the liquid will be displaced between the parallel plates and creates a laminar flow [6]. For the two-plate-model, only laminar flow is applicable, as turbulent flow regimes would increase the models flow resistance, thus showing false rheological properties.

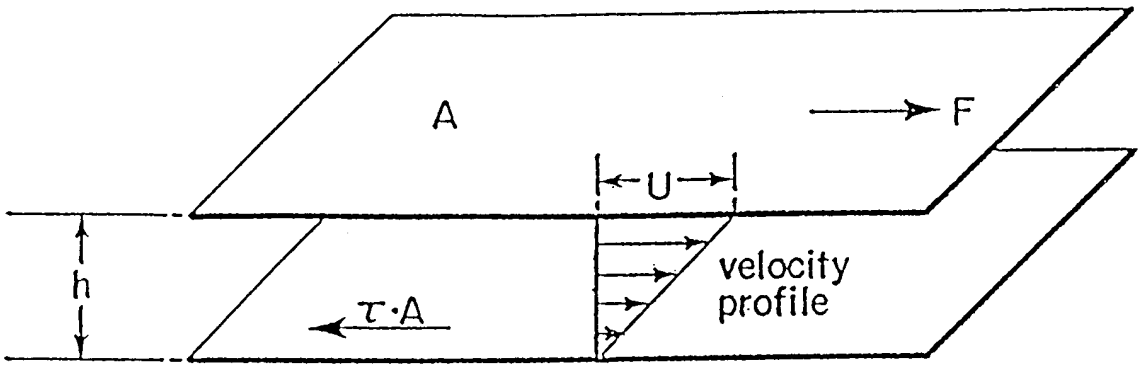

Figure 2: Principal of the Two-Plate Model for rheological measurements. Velocity distribution and shear arte in the shear gap [7]

Shear stress (τ) and shear rate describe the behavior within the two-plate-model. Shear stress is a measure of the force from a fluid acting on a body in the path of that fluid and is calculated as follows:

$$\tau = \frac{F}{A} \qquad \text{(EQ 1.2)}$$

Here, F is the Force acting on area A to effect a movement in the liquid element between the two plates. The velocity of the movement at a given force is controlled by the internal forces of the material [8]. Units are denoted as Newton [N] for the acting force and [m^2] in respect of the area, which results in Pascal [Pa] being the unit for shear stress.

The principle describing shear rate, is that a laminar shear flow is generated between the two plates if shear stress is applied. The uppermost layer moves at the maximum velocity v_{max} , while the lowermost layer remains at rest. This principle was explained earlier in this chapter.

In mathematical terms, the shear rate can be written as;

$$\gamma = \frac{dv}{dh} \qquad \text{(EQ 1.3)}$$

Where, *dv* is the velocity differential between adjacent velocity layers and *dh* is the thickness differential of the flow layers. The unit of shear rate is [1/s] or also [s^{-1}], referred to as 'reciprocal seconds' [6]. The velocity differential between adjacent layers of thickness is constant in a two-plate system without the influence of pressure and for constant viscosity.

The differential can thus be approximated as follows:

$$\gamma = \frac{v}{h} = \frac{m/s}{m} = s^{-1} \qquad \text{(EQ 1.4)}$$

with *v* being the velocity and *h*, the distance in respect of each layer.

1.2.3 Dynamic viscosity

For a laminar flow of a fluid, the ratio of the shear stress to the velocity gradient is perpendicular to the plane of shear. Simply, viscosity describes the ruggedness of a given material and can be mathematically termed as follows [9];

$$\eta = \frac{\tau}{\gamma} = \frac{Pa}{s^{-1}} = \text{Pas} \qquad \text{(EQ 1.5)}$$

Dynamic viscosity is described by η.

1.3 Load – Dependent Flow behavior

1.3.1 Newtonian Flow

It is commonly known that the viscosity coefficient η is defined as the ratio of the shear stress τ to the rate of shear γ. A fluid is then called Newtonian if the viscosity coefficient is independent of the rate of shear. Hence the mathematical term for Newton's law of viscosity is as follows;

$$\tau = \eta * \gamma \qquad \text{(EQ 1.6)}$$

Shear stress has units of pressure, [$1N/m^2$ = 1 Pa] and the shear rate units of [s^{-1}]. Therefore, the viscosity, which is the ratio of the shear stress to the shear rate, has units of Pa-s. One can also say that Newtonian fluids have direct proportionality between shear stress and shear rate in laminar flow [11].

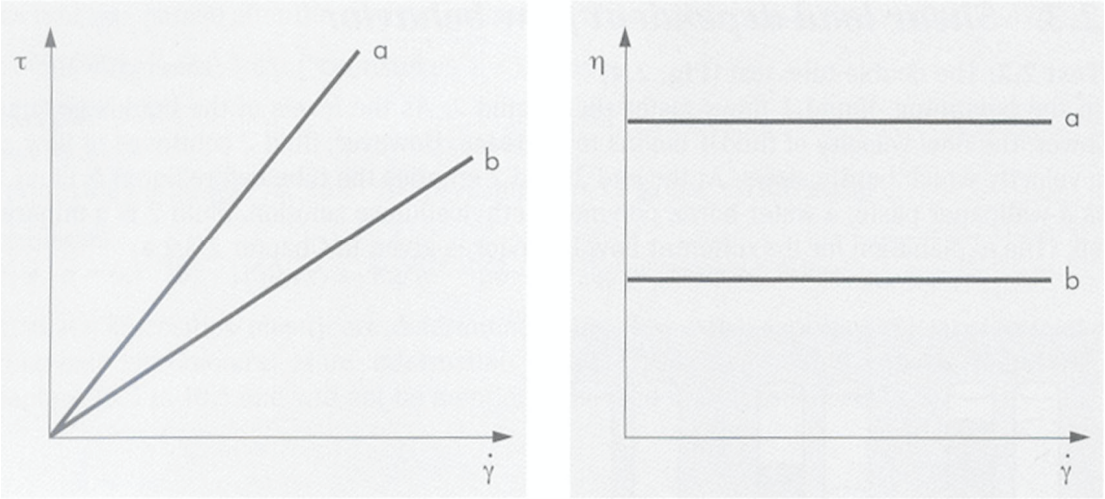

Figure 3: On the right; flow curves of two idealviscou fluids; left side shows viscosity curve of two idealviscous fluids [6]

η is the material constant of the dynamic shear viscosity. If the viscosity is plotted over the shear rate, or shear stress for that matter, in a viscosity diagram, a straight line which starts at $\gamma = 0\ s^{-1}$ (or $\tau = 0$ Pa) and runs parallel to the abscissa is obtained for an ideally viscous material [12].

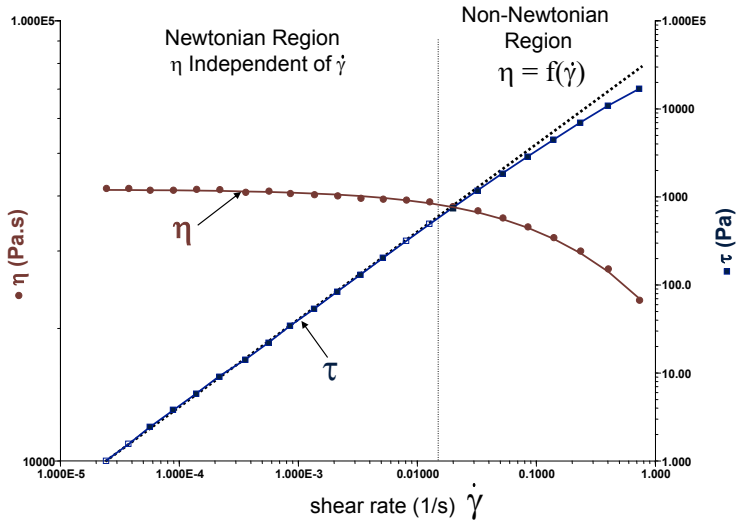

Figure 4: Behavior of Newtonian and non-Newtonian fluids in respect of each other [13]

The Rheology of many simple materials such as pure liquids, solutions of solutes smaller than macromolecules, and even some polymer solutions can be characterized as Newtonian. In general they are low-molecular liquids showing a molar mass below 10,000 g/mol [6].

Nevertheless, a great variety of liquids used in everyday life are non-Newtonian. Examples include ketchup and mustard, paints, margarine and ointments. These liquids cannot be defined by a single viscosity value at a specified temperature.

1.3.2 Non-Newtonian Flow

Numerous researchers in the field of rheology have long classified non-Newtonian fluids as plastic, pseudoplastic, dilatant, thixotropic, and a few others, having found the foregoing divisions unsatisfactory, have added “general non-Newtonian” classifications [14].

The classification of fluids into those categories mentioned, gives a gross oversimplification of the facts. It has repeatedly been shown that the classification into which a fluid is categorized, and even the numerical values assigned its rheological properties, is extremely dependent upon the experimental conditions under which the measurements are made [15,16].

In the past 50-60 years, there has been a growing recognition of the fact that many substances of industrial significance, especially of multi-phase nature (foams, emulsions, dispersions and suspensions, slurries, for instance) and polymeric melts and solutions (both natural and man made) do not conform to the Newtonian postulate of the linear relationship between τ and $\dot{\gamma}$ in simple shear, for instance. Accordingly, these fluids are variously known as non-Newtonian, non-linear, complex, or rheological complex fluids [17].

The non-Newtonian fluid behavior in nature and in technology is so widespread, that it would be no exaggeration to say that the Newtonian fluid behavior is an exception rather than the rule!

This chapter endeavors to provide a brief introduction to the different kinds of non-Newtonian flow characteristics, their characterization and implications in engineering applications.

1.3.2.1 Pseudoplasticity

If the shear rate grows, many materials show a strong decrease in viscosity. This effect is of great technical importance. Compared with an ideally viscous material, a pseudoplastic or structurally viscous material can be pumped through pipelines with a lower energy input at the same flow velocity.

Also known as shear-thinning flow behavior, their meaning is identical, however 'pseudoplastic' contains the word 'plastic', a behavior which cannot be exactly determined in a scientific sense since it is the result of inhomogeneous deformation and flow behavior [6].

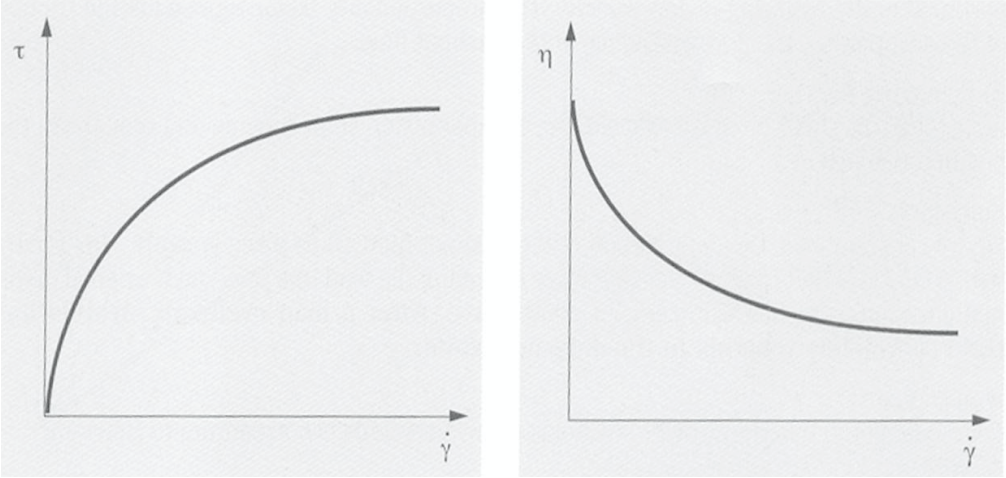

Figure 5: left: flow curve of a shear-thinning material, right: viscosity curve of a shear-thinning material [6]

The proportionality factor τ / γ in the Newtonian constitutive equation is thus referred to as η_a. Hence, η_a is the apparent viscosity and denotes the viscosity at a certain shear rate γ.

$$\frac{\tau}{\gamma} = \eta \neq const. \qquad \text{(EQ – 1.7.)}$$

Materials are referred to as pseudoplastic or shear-thinning, if a force acting on the body causes the particle size to change, the particles to be oriented in the direction of flow, or an agglomerate to be dissolved [18].

1.3.2.2 Dilatancy

This class of fluids is similar to pseudoplastic systems in that they show no yield stress, but their apparent viscosity increases with the increasing shear rate and hence the name shear-thickening [17]. Here a leading example would be stirring in wet sand. In 1885 Reynolds created the term 'dilatancy' to describe the effect of round sand particles, all of which have roughly the same size, and are completely wetted by sea water. The then experienced difficulty in stirring this mixture is caused by the obstruction of flow of a closely packed and deflocculated system of particles [19].

Reynolds explained this phenomenon with the occurrence of undisrupted sand particles settling to a close packed arrangement and that any disturbance causes rearrangement to a smaller number of nearest neighbors, in which the particles are farther apart.

The viscosity of dilatant materials also depends on the shear rate. It increases as the shear rate grows. Dilatant behavior can cause trouble in technological processes, and it is mathematically expressed according to Ostwald De Waele [12];

$$\tau = K * \gamma^{n} \qquad \text{(EQ – 1.8)}$$

where *n* greater 1 (n >1) stands for dilatant material. This can be transformed into a viscosity function as follows;

$$\eta = \frac{\tau}{\gamma} = K * \gamma^{n-1} \qquad \text{(EQ – 1.9)}$$

The exponent n is known as the Power Law Index or Ostwald De Waele Law. For a shear thinning fluid: 0<n<1. The more shear-thinning the product, the closer n is to zero [12].

One has to also acknowledge that in the case of high shear rates the flow in the measuring gap is no longer laminar, but becomes turbulent, this may falsely suggest dilatant behavior [20].

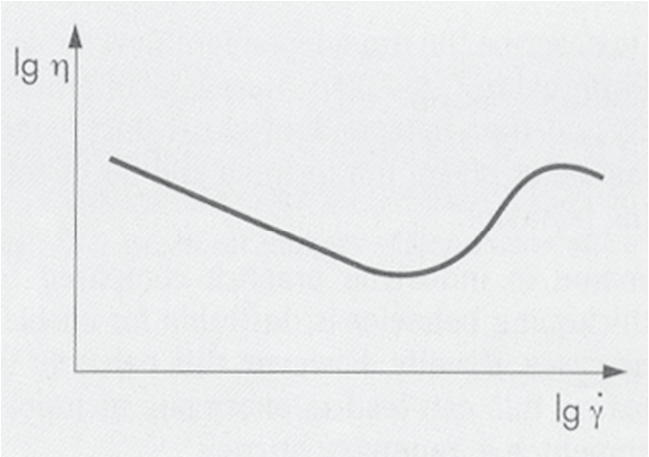

Figure 6: Viscosity curve for a material with dilatant behavior [6]

1.3.2.3 Plasticity and yield point

Generally speaking, in Physics, Plasticity is known to describe structurally viscous liquids, which have an additional yield point, called τ_0. A practical example for a specific material showing such properties is toothpaste. At rest, toothpaste establishes a network of inter molecular bonding forces. These forces prevent individual volume elements to be displaced when the material is at rest. Now, if an external force, which is smaller than the internal force acts on the material, the resulting strain is reversible.

However, if the external forces exceed the internal bonding forces of the network, the material will start flowing, the solid turns into a liquid [12].

In the past, three dedicated scientists approximated definitions to find a mathematical expression and flow curves for materials with a yield point. Bingham was the first to create such a mathematical model;

$$\tau = f_B + \eta_B * \gamma \qquad \text{(EQ – 1.10)}$$

where f_B is the yield point according to Bingham's theory [21].

Flow curves of plastic liquids do not start in the origin of the coordinated system, but run on the ordinate axis until the yield point τ_0 is reached, then they converge from the ordinate.
Various equations are used to mathematically express the flow curves, which is then dependable of the actual material.

For example, the curves expressed for the flow of chocolate is typically based on the Casson model;

$$\sqrt{\tau} = \sqrt{f_c} + \sqrt{\eta_c * \gamma} \qquad \text{(EQ – 1.11)}$$

where f_C is known as the yield point according to Casson. [22]

The last mathematical expression in this regard was produced and manifested by Herschel and Bulkley [23]. The equation is approximated as follows;

$$\tau = f_H + m * \gamma^p \qquad \text{(EQ – 1.12)}$$

in this formulation, f_H is the yield point according to Herschel und Bulkley.

1.3.3 The Carreau Model

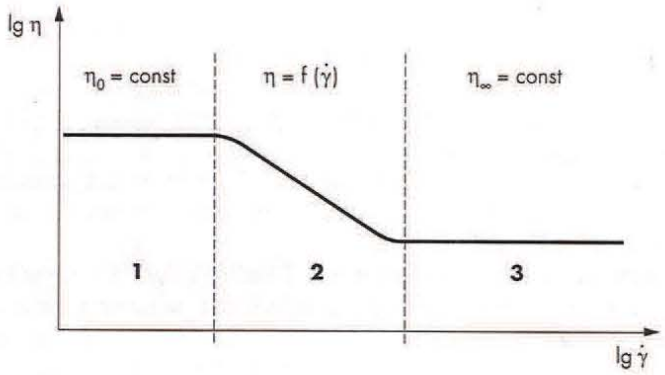

Figure 7: Viscosity function of a polymer [6]

Figure 7 shows the viscosity function of a polymer depicting three ranges on a double logarithmic scale [6].

1. The first Newtonian range with the plateau value of the zero-shear viscosity η_0.
2. The shear-thinning range with the shear rate-dependent viscosity function $\eta = f(\gamma)$
3. The second Newtonian range with the plateau value of the infinite-shear viscosity $\eta\infty$.

Diagram areas (1) and (2), the model function for zero-shear and rate-dependent viscosity, are relevant for the work presented in this Thesis and is mathematically described through the Carreau model, which is approximated as follows:

$$\frac{\eta - \eta_\infty}{\eta_0 - \eta_\infty} = \frac{1}{\left(1 + \left(\frac{\dot{\gamma}}{\dot{\gamma}_{crit}}\right)^a\right)^{m/a}} \qquad \text{(EQ – 1.13)}$$

Here, η_0 is the zero shear rate viscosity, η_∞ the infinite shear rate viscosity, $\dot{\gamma}_{crit}$ the critical shear rate, *m* the Carreau index. The exponent *a* is equal to *'2'* in the original Carreau model.

1.4 Time-dependent Flow behavior

1.4.1 Thixotropy

If we go back in history, the term thixotropy was originally coined to describe an isothermal, reversible, solid-liquid transition due to mechanical agitation.

In 1923, Schalek and Szegvari (which was translated and reviewed by Bauer and Collins et al.) found that aqueous iron oxide gels have the remarkable property of becoming completely liquid through gentle shaking alone, to such an extent that the liquefied gel is hardly distinguishable from the original sol [24]. Nowadays, thixotropy is referred to as the continuous decrease of apparent viscosity with time under shear and the subsequent recovery of viscosity when the flow is discontinued. The material is assumed to be at rest for a sufficiently long time before the said experiment is performed [25].

The opposite effect also exists, and is known as antithixotropy or rheopexy [26]. However, Thixotropy is a property exhibited by non-Newtonian liquids, they return to their original viscosity only with a delay after the shear force ceased to act. In addition, these materials often also have a yield point. A perfect example here would be Tomato ketchup. When stirred it becomes thinner and only returns to its original viscosity after allowing resting for a while.

On the other hand, yoghurt serves as a counter-example as it shows irreversible thixotropic behavior, becomes thinner when stirred but does not return to its original thickness [25].

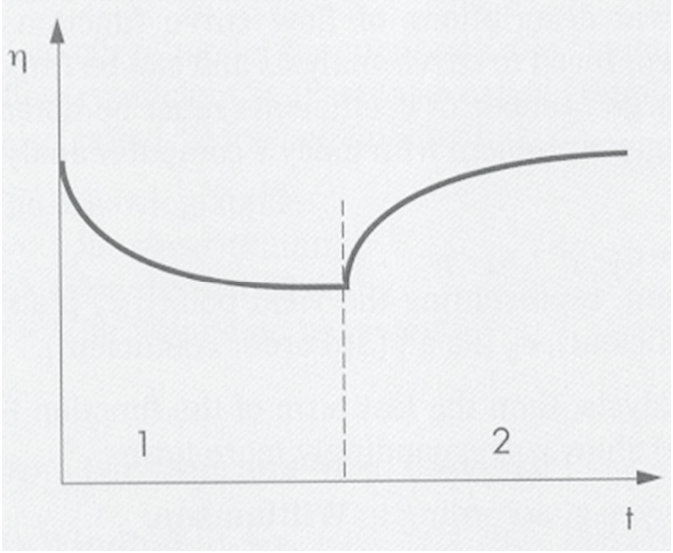

Figure 8: Viscosity time curve of a thixotropic material [6]

Two transitional areas can be easily identified in the viscosity-time curve shown in Figure 8. Part (1) depicts time-dependent decomposition under constantly high shear; part (2) time-dependent structural regeneration when at rest.

1.4.2 Rheopexy

Another kind of Non-Newtonian behavior, which was briefly mentioned before, can be made manifest by the stirring at constant shear. The viscosity builds up in time, creating a structure that is unable to relax instantly. This effect is the opposite of the aforementioned thixotropic effect [11].

However, Freundlich created the term 'rheopexy' for this very phenomenon, commenting, "it is too cumbersome to say 'thixotropic sols that can be solidified by orienting the particles'" [27].

Rheopectic materials are considered to exhibit greater viscosity while they are subject to shear stress. Structures are established in the material during the application of mechanical shear forces. "The original viscosity is only restored with a delay after the shear forces ceased to act on the material, by disintegrating this structure"[12].

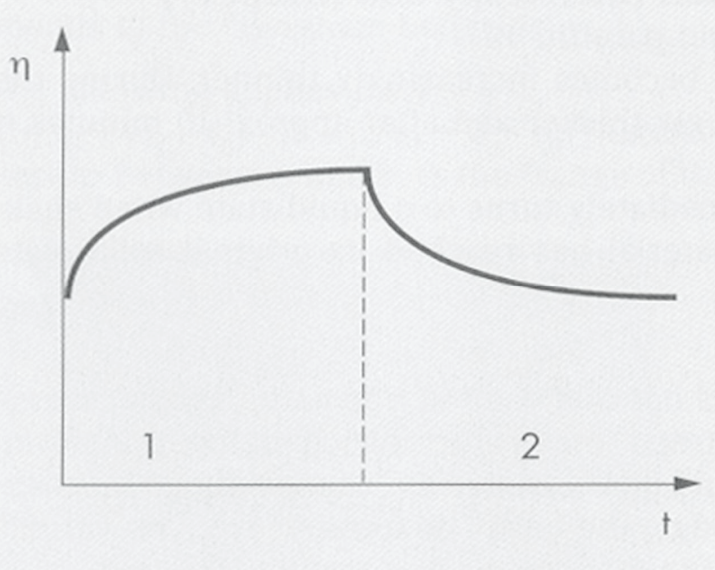

Figure 9: Viscosity time curve of a rheopectic material [6]

Figure 9 is explained in two parts; Part (1) depicts time-dependent increase in structural strength under constantly high shear load; Part (2) shows time-dependent decrease in structural strength when at rest.

After various research and test stands created in the past, one can assume that this process of viscosity increase and decrease can be repeated as often as one wish. But in contrast to thixotropy, true rheopexy is very rare [27-30].

As was noted in this chapter, time-independent fluid behavior can exist in three different types that are all described by their steady shear behavior. One distinguishes between;

1. Shear-thinning behavior (pseudoplastic)
2. Visco-plastic behavior with or without shear-thinning behavior
3. Shear-thickening behavior (dilatant)

The flow curves, or rheograms for different types of non-Newtonian fluids is visualized and compared in Figure 10.

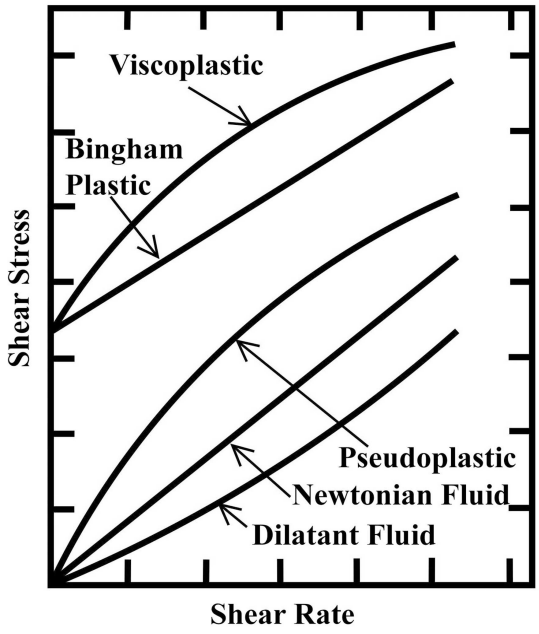

Figure 10: Comparison of non-Newtonian fluid behavior [17]

1.5 Viscoelasticity – the Maxwell Model

Viscoelasticity is a time-dependent mechanical response to loading exhibited most often by amorphous materials. Furthermore, it is known that viscoelastic materials always show both, viscous and elastic behaviors, simultaneously [6]. The Elastic part behaves according to Hooke's Law, whereas the viscous part behaves according to Newton's law. Voigt proposed the very first model; it is good but is unable to describe the commonly observed relaxation of stress in strained viscoelastic materials.

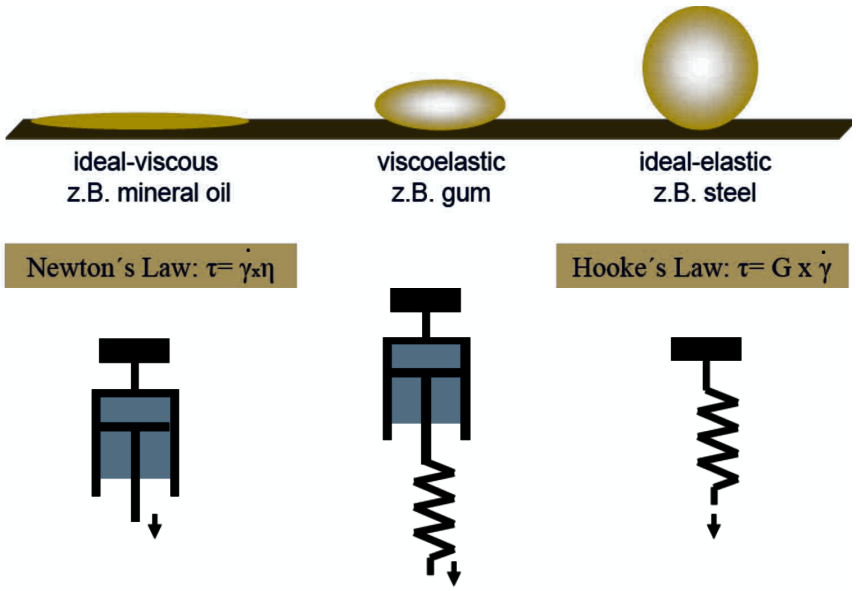

Figure 11: Maxwell model of VE [31]

The model, created by James C. Maxwell that illustrates this behavior of viscoelastic liquid can be seen in Figure 11. The simplest models of viscoelastic constitutive behavior result from a linear combination of elastic and viscous behavior.

Elastic behavior is represented by a spring while viscous behavior is represented by a dashpot. In the Maxwell model the spring and dashpot are connected in series so that they experience the same stress [12].

CHAPTER II

2. Instruments

2.1 Apparatus Design of Rheometer models

This chapter is supposed to give an overview of the two major types of Rheometers in use for testing rheological properties. Capillary Rheometers, also known as Viscometers and Rotational Rheometers are introduced. Rheometers are instruments for measuring rheological properties of liquids and soft matter. Typical rheological properties are viscosity, storage and loss modulus, compliance, yield stress, and relaxation times [12]. These properties depend on the microstructure of the material and, hence, depend on stress or strain-induced structural changes, and on time.

2.2 Capillary Rheometer (Viscometer)

Traditionally, capillary Rheometers have been used to measure the shear viscosity and elasticity of viscous materials at high shear rates. More recently, extensional viscosity has been obtained through the work of Cogswell et al [32]. F.T. Trout was the first to introduce the term extensional viscosity, described as “coefficient of viscous traction”. The relation between extensional viscosity η_E and shear viscosity η is discussed. However, researchers argue whether his concept actually causes more confusion then enlightenment [33]. The interest in high shear rates stems from the mode of deformation a material will undergo in processes like extrusion, film blowing, and injection molding. The design and operational principle of a capillary rheometer are conducive to providing rheological data under these unique processing conditions. The moving piston/die arrangement produces high shear rates on the order of 10^7 s^{-1} [34].

A measure of elasticity can be determined by measuring expansion of the sample at the die exit, called die swell. Melt fracture can be studied by observing the extrudate. As a result, capillary Rheometers are widely used in both research environments and quality control laboratories [34].

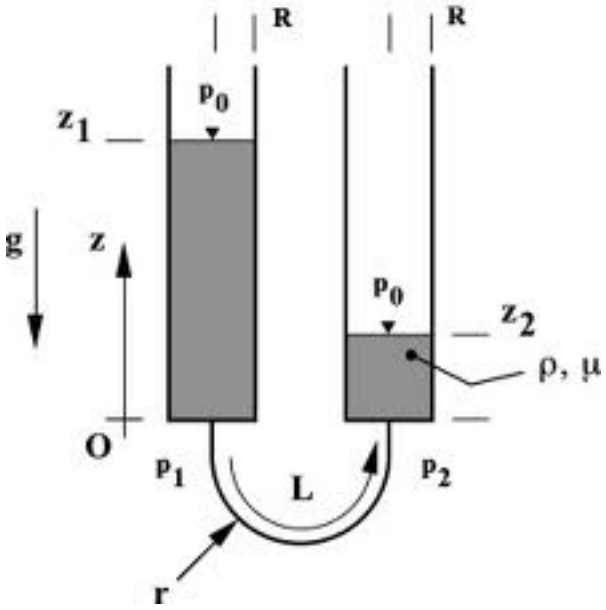

Figure 12: capillary viscometer [35]

In figure 12 the theoretical set up of a capillary viscometer is explained. The length of the communicating capillary is L [cm], and the inner radius is represented by r. The dynamic viscosity and the mass density of the liquid are μ [N s/m^2] and ρ [m/V], respectively. The acceleration due to gravity is *g*. A steady-state, uniform temperature is assumed for the entire viscometer [35].

Furthermore, capillary Rheometers suffer from several limitations when attempting to measure fluids with viscosity lower than 1 Pa s:

1.) *Sample flow by gravity through the traditional vertical capillary die when no instrument driving force is applied;*

2.) *Low-pressure readings from the transducer during the measurement;*

These limitations however are not applicable for highly viscous substances described later in this work. Many times the measured pressure signal can reach the low-end limit of the pressure transducer used. Dao and Ye [34] also mention a concern with required length-to-diameter ratio of the die for the measurement to be rigorous.

Figure 12: State of the art CR-6000 Capillary Viscometer [36]

The Canadian based testing institution, 'Qualitest International Inc.' describes in one of their dossiers for a capillary viscometer that, "It is specially designed to determine the flow behavior and viscosity of high polymers, polymers, thermoplastics and elastomers. This single bore instrument will provide reliable data and a unique data point range for QA and R&D purposes" [37].

2.3 Rotational Rheometer

Rotational Rheometers can be used to determine transient and steady shear flow properties of materials. This typically includes; shear viscosity, creep or stress relaxation.

The principle, and often the instrument, is the same as for the oscillatory Rheometer, except that the deformation of the sample is obtained by rotating rather than oscillating one plate relative to the other [38]. Furthermore, rotational Rheometers are widely utilized in oscillatory shear mode to characterize linear viscoelastic fluid properties, in terms of the storage and loss modulus, G' and G'', respectively.

For tests with controlled shear strain in the form of oscillatory sine functions, one estimates:

$$\gamma(t) = \gamma_A * \sin \omega t \qquad \text{(EQ – 2.1)}$$

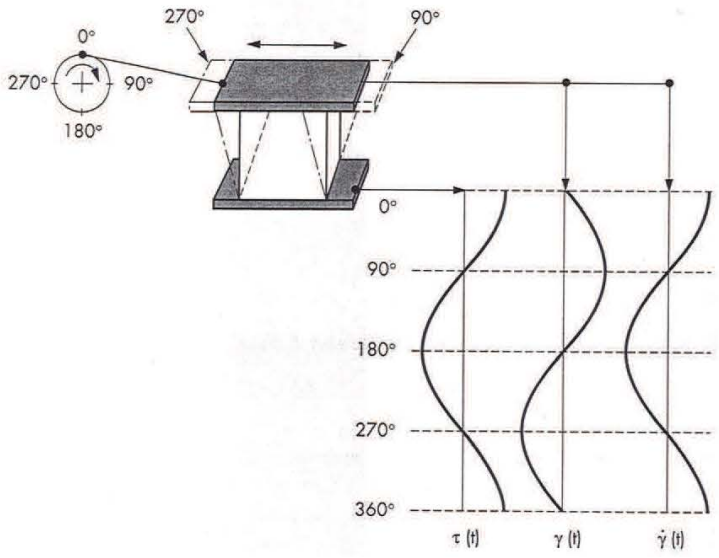

Figure 13: The sine and cosine curves of the time-dependent functions for idealviscous behavior [6]

The storage modulus G' is a measure for deformation energy stored by the analyzed sample during the shear process [6]. The energy is completely available, acting as the driving force after the load is removed, for the reformation process. This partially or in its entity compensates the previously obtained deformation of the structure [39]. Materials storing the whole available energy are known to show completely reversible deformation behavior. This is attributed to their unchanged shape after the load cycle [6]. This postulates that the storage modulus G' represents the elastic behavior of a tested substance.

On the other side, the loss modulus G" measures the deformation energy used up by the sample during the shear process [6]. In layman terms this refers to the energy loss of the sample. The energy is spent during the deformation of the sample's structure. These types of energy losing materials show an irreversible deformation behavior [39]. This is accounted by their change of shape during the load cycle [6]. The loss modulus G" represents the viscous behavior of a tested substance.

In this work a rotational Rheometer was used to analyze properties of pharmaceutical polymers, such as Soluplus®. Now this Chapter will emphasize on the basic fundamentals of a rotational Rheometer.

Overall, several different measurement systems are known to be used in conjunction with a rotational Rheometer. In this case study, which is presented here, only the Cone-Plate and Plate-Plate systems were used.

2.3.1 Cone-Plate System

The cone-plate apparatus consists of a shallow rotating cone on top of a stationary plate, both attached to a circular cylinder [38]. The test stand provides a rapid means of obtaining reproducible flow measurements on Non-Newtonian fluids by subjecting the sample to definite uniform shear stress due to a fixed gap.

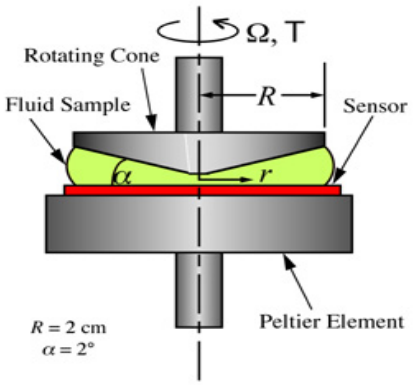

Figure 14: Cone-Plate measuring system for a Rotational Rheometer [40]

A sample is placed between the plate and cone of the representative system. When the angle between the cone and plate is very small and the rotational speed is low, the flow is basically azimuthal, meaning that streamlines are concentric circles, the velocity profile is linear and the shear-rate is constant, like in Couette flow [41].

Azerat and Baensch suggested in their work that the exhibited flow pattern in a cone-plate measuring system is only approximately azimuthal, as the angle and rotational rate increases, the fluid near the cone experiences an increasing centrifugal force that promotes radial fluid motion towards the periphery of the device [41].

They manifest that a radial secondary flow develops here, where the streamlines turn into spirals until the onset of turbulence. This phenomenon was first observed by Cox et al. and later on manifested by Fewell and Hellmus [42, 43].

The Cone-plate model is mainly used for very viscous or viscoelastic materials. The Cone-Plate system is also widely used in the food industry to control the viscosity of certain food products. Nevertheless, it does hold certain restrictions due to the fixed measuring gap when analyzing suspensions. To elude this problem, the plate-plate system offers a useful alternative.

2.3.2 Plate-Plate System

In contrary to the cone-plate measuring system, the plate-plate system offers a wide range of measurement parameters with small errors due to an adjustable gap. This gives great advantage when analyzing suspensions, as the gap can be customized to account for various particle sizes yielding to sound results with a far lower range for errors.

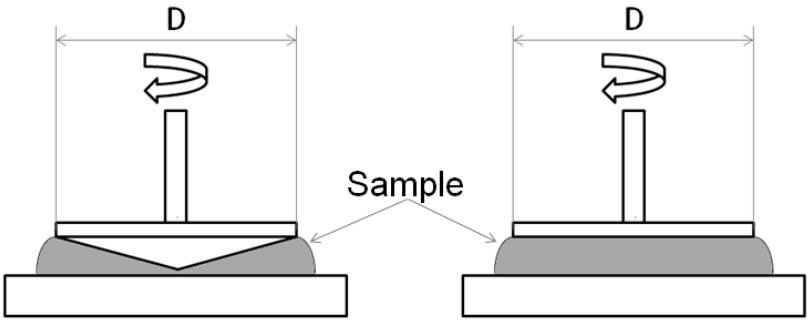

Figure 15: Compares the geometries of a Cone-Plate and a Plate-Plate model [3]

2.4 Test procedure with a rotational Rheometer

2.4.1 Amplitude Sweep

Amplitude sweeps, also known as dynamic stress sweeps, belong to the range of oscillatory tests performed at variable amplitudes but keeping the frequency and temperature at constant value [6]. The test is used to determine the linear viscoelastic range (LVE) limitations over a stress or strain range. The results can often give an indication of material stability.

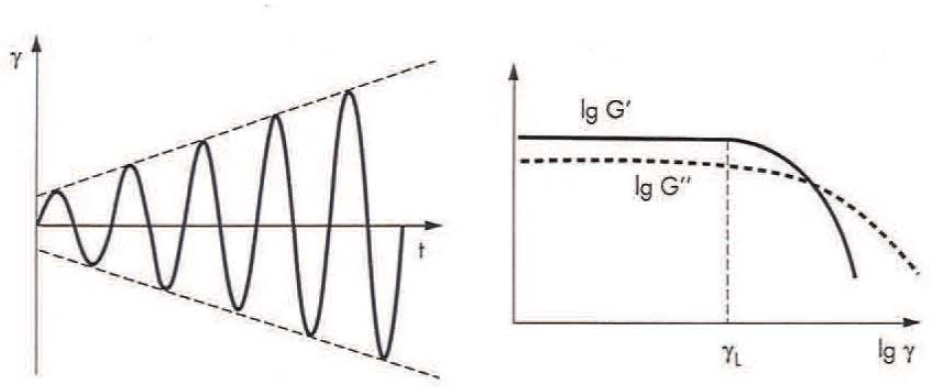

Figure 16: Amplitude Sweep [6]

The wider the linear viscoelastic range the more stable the material. While sample structure is maintained, the complex modulus is constant. When the applied stress becomes too high, breakdown occurs and the modulus decreases [12]. Meaning if the LVE is much shorter, the break down is more evident and easier reached.

2.4.2 Frequency Sweep

Frequency sweeps, like the amplitude sweep, are oscillatory tests that are performed at variable frequencies but keeping the amplitudes and measuring temperatures at constant value.

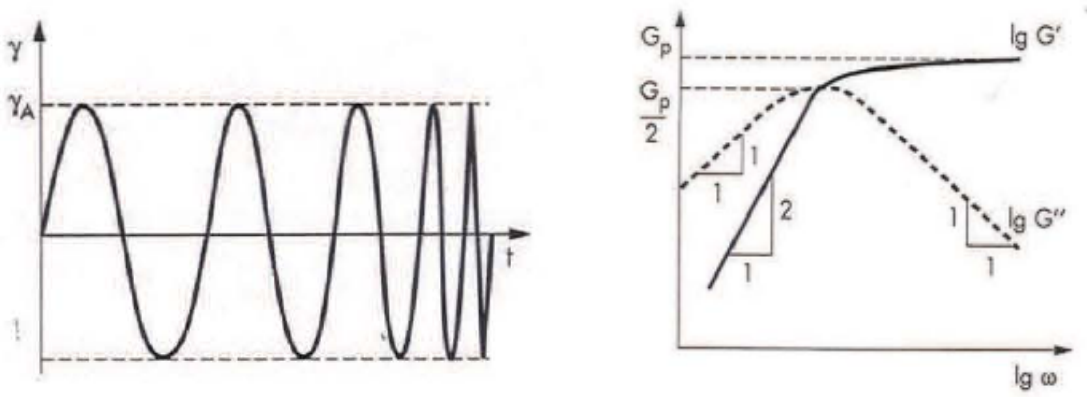

Figure 17: Frequency Sweep [6]

A frequency sweep is a particularly useful test as it enables the viscoelastic properties of a sample to be determined as a function of timescale. So generally speaking it investigates time-dependent shear behavior, since the frequency is the inverse value of time. Short-term behavior is simulated by rapid motion, at high frequencies and long term behavior by slow motion, hence at low frequencies [6]. Several parameters can be obtained, such as the storage elastic-modulus G', the viscous loss-modulus G", and the complex viscosity η*. The storage modulus can be used as a measure of the elastic component of the sample and similarly, the loss modulus, the viscous component of the sample [44].

The complex viscosity can be determined during forced harmonic oscillation of shear stress and is referred to as a frequency dependent-viscosity function. It is related to the complex shear modulus and represents the angle between the viscous stress and the shear stress [61]. The complex viscosity function is equal to the difference between the dynamic viscosity and the out-of-phase viscosity, or imaginary part of the complex viscosity. This can be mathematically approximated from Pythagoras theorem as follows [62]:

$$|\eta^*| = \sqrt{(\eta')^2 + (\eta'')^2} \qquad \text{(EQ – 2.2)}$$

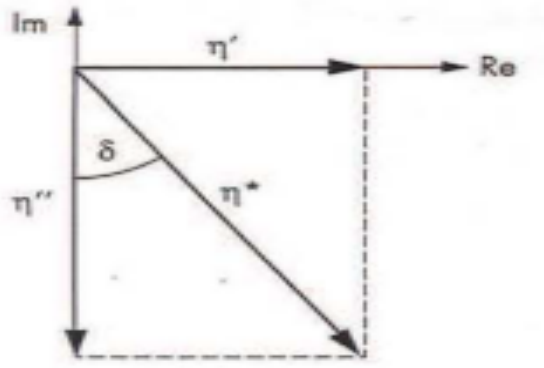

Figure 18: Vector Diagram of complex viscosity function [6]

To describe the relations in equation 2.2; η^* is the complex viscosity, η' is the in-phase viscosity and η'' is the out of phase viscosity. However some use the term η to describe the complex viscosity in the regard of oscillatory measurements derived from Cox-Merz rule; which holds that: $\eta(\gamma) = |\eta^*\gamma|$, for γ [1/s] equals ω [1/s], and refers to the theory of the complex viscosity being identical to the shear viscosity if the angular frequency is replaced by the shear rate [10]. This rule is applicable for most polymer melts and oscillatory tests involving a frequency sweep.

2.4.3 Temperature Test

The temperature sweep provides the dependency of viscosity and insight of the materials melt strength. Also, when a low frequency is used, i.e. 1 rad/sec, the test is very sensitive to branching, both long and short, and the materials structure [6]. This sweep test rather focus on a temperature/time-profile then on measurement parameters in respect of frequency or amplitude. In the Rheogram the storage modulus G' and loss modulus G" in respect of temperature is depicted.

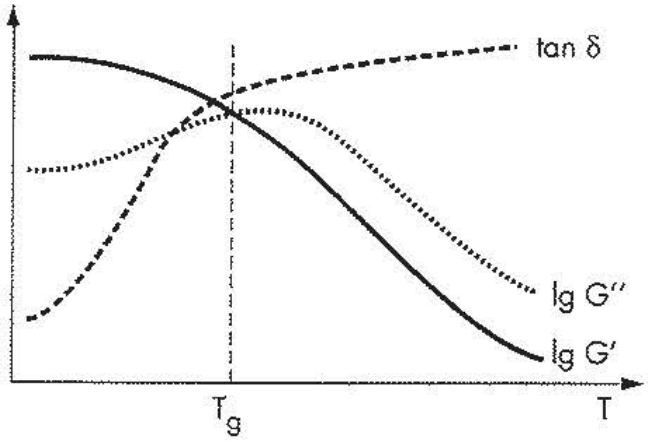

Figure 19: Temperature-dependent functions of G' & G" [6]

The value for the glass transition temperature T_g can vary considerably depending on various details of the experimental technique. This value can only be seen as an estimate; hence it's not a 'sharp' temperature point [6]. For example, the softening range of the Soluplus® Polymer covers a wide temperature range which easily covers: ΔT = 70-80°C. Therefore, T_g is dependable on the heating or cooling rate as well as on the test frequency.

Chapter III

3. Polymers

3.1 Adhesion Phenomena

The process that allows the adhesive to transfer a mechanical stress from the adherent to the adhesive joint is known as the adhesion. It is the interatomic and intermolecular interaction at the interface of two surfaces. Nowadays it does not only include physics but belongs to an interdisciplinary field comprising of surface chemistry, rheology, polymer science and material science, stress analysis, fracture analysis and of course last but not least, physics. [47]

The ultimate researcher's goal is to identify a single mechanism that explains adhesion phenomena, but due to the complexity and evolving understanding of the subject, this seems rather unrealistic. Adhesion mechanisms have been known to be dependent on the surface characteristics of the materials in question since the early beginnings of both the aerospace and automobile industries. Since then, and especially in the last 30 years, the understanding of adhesion mechanisms has increased significantly as both industries have sought lighter and cheaper alternatives to metals and metal components.

This drive has been the major influence in the need to understand polymer adhesion and to resolve the debate over how the interfaces are actually adhering [48-50].

3.2 Adhesion of Polymers

Adhesion is acknowledged to be one of the more complex subjects to describe in simple terms. Adhesion to and by polymers is a particularly subtle part of the subject, and one of increasing applied importance. The subtlety lies in the many characteristic properties of polymer surfaces and interfaces.

In the last three decades, the level of basic adhesion research has outnumbered the growing use of the technological applications, in industry as well as applied sciences. Despite this, a single unifying theory that adequately describes all adhesion phenomena is yet to be proposed. However, several basic models have been established. The following mechanisms of adhesion are emphasized and discussed in five subchapters:

- Mechanical Interlocking
- Electronic Theory
- Diffusion Theory
- Molecular bonding
- Adsorption Theory

3.2.1 Mechanical Interlocking

Mechanical interlocking is a theory that essentially proposes mechanical keying, or interlocking, of the adhesive into the irregularities of the substrate surface, which is the major source of instrinsic adhesion [51]. F. Awaja et al. discusses some theories on mechanical interlocking that had been treated by researchers through the past decade. He states that observation of abrasive treatment of smooth solid surfaces in the presence of an adhesive may increase the strength of the adhesive joint. However, in theory, the destruction of the surface may allow for the formation of macro radicals, and hence an increase in chemical bonding sites [48].

Although a number of examples relating joint strength and durability to increased surface roughness exist in literature, the theory is not universally applicable since good adhesion occurs between smooth surfaces, such as the adhesion that occurs between wet glasses microscope slides. K.W. Allen et al. observed that increased roughness could result in lower joint strengths [52]. Mechanical interlocking can make a significant contribution towards the joint strength if the adherent surface geometry is specifically fabricated to enhance adhesive penetration.

On the other hand, F. Awaja et al. debates on opposing the mechanical interlocking theory, as many other researchers have noted the significance of mechanical interlocking in explaining adhesion phenomena but in combination with other forces [48]. Brown et al. found that adhesion between surfaces is influenced by the presence of van der Waals forces in addition to mechanical coupling. Furthermore it was noted, that these forces are not sufficient to create the strong interfacial bonding observed between polymers [53].

Other research groups have studied the importance of the surface porosity in the mechanism of adhesion. The work of Packham et al. suggests that the shape of the pore, is a crucial factor in controlling the pore filling process [54].

Subsequently, penetration of the adhesive into pores on the surface can contribute significantly towards high joint strengths, since it is believed that the adhesive that penetrates into the pores requires considerable plastic deformation, and thus high fracture energy.

3.2.2 Electronic Theory

K. Ananchaorengwong describes in his work that this theory postulates that adhesion arises from the interaction of point charges, positive and negative, on either side of an interface, where on one side there is a solid, and on the other an electric double layer composed of solvated ions and counter-ions. This model finds much application in colloid science [55].

3.2.3 Diffusion Theory

The diffusion theory concept was described by Wool et al. as the penetration of adhesive into the substrate. The diffusion theory of adhesion proposes that adhesion can be attributed to the interdiffusion of polymer molecules at the interface [56].

Voyutskii et al. postulates that the adhesion between two polymers is a result of interfacial interdiffusion of polymer chains [57]. However, numerous researchers, such as Allen et al. criticize the theory in regard that if the interdiffusion process is involved, the joint strength should depend on the type of the material, contact time and pressure, temperature, molecular weight, and formation of primary and secondary interfacial forces [58].

3.2.4 Molecular Bonding

This theory is by far the most widely accepted mechanism for explaining adhesion between two surfaces in close contact. It entails intermolecular forces between adhesive and substrate such as dipole-dipole interactions, van der Waals forces and chemical interactions, that is, ionic, covalent and metallic bonding. This mechanism describes the strength of the adhesive joints by interfacial forces and also by the presence of polar groups. [59]

It is understood, that molecular bonding mechanisms require an intimate contact between the two substrates. However, intimate contact alone is often insufficient for good adhesion at the interface due to the presence of defects, cracks and air bubbles [60]. The molecular bonding mechanism is a subject that is not yet fully understood and there have been many theories proposed to explain it.

For example, Mutsuda and Komada studied poly(oxy- 2,6-dimethyl-1,4-phenylene) (PPE) bonding to rubber. The group reported that the adhesion mechanism was based on a hydrogen abstraction reaction. This occurs when the separation between two polymer substrates becomes negligible, allowing radicals from one substrate to attack the other causing the formation of more radicals. Subsequent recombination of these radicals with the polymer allows chemical bonding between the substrates [61].

Bailey and Castle as well as Kinloch et al. brought further evidence for this hypothesis with their work conducted in the X-ray photoelectron spectroscopy (XPS) and Time-of-Flight Secondary Ion Mass Spectrometry (ToF-SIMS) field [62, 63]. It was shown that interfacial bonding was the crucial factor in the adhesion strength between silanes and metals.

Basin et al. reports another theory in his research article, which considers adhesion between solid substrates and organic coatings. They reported that as the number of chemical bonds increased at the contact zone, adhesion strength passed through a

maximum value [64]. This finding is supported by the study investigating the shear strength of aluminium– polypropylene lap joints by Chen *et al*. [65]. Chen et al. found that the overriding adhesive mechanism was the chemical interaction between the functional groups at the interface and also concluded that excessive chemical bonding at the adhesive interface could have a negative effect on the interface strength. This hypothesis supported several other studies that circulated that time.

Furthermore, they showed that adhesion strength has been shown to depend on the thickness of the adhesive layer for composite interfaces. Interfacial bonding strength increases as the thickness of the adhesive layer is reduced, as stress is able to dissipate through the interface much easier [66].

3.2.5 Adsorption Theory

According to Allen et al. adhesion by this mechanism is attributed to surface chemical forces, and the chemisorption or physisorption of atomic and molecular species. The attractive forces working across two surfaces include weak dispersion forces and stronger forces due to hydrogen, covalent, and ionic bonding [52]. This is also known as the thermodynamic adsorption model of adhesion. However, on the contrary Lipatov et al. argues that the advantage of this mechanism, over others is that it does not require a molecular interaction for good adhesion, only an equilibrium process at the interface. In neutral environments such as air, the thermodynamics of the polymer system will attempt to minimize the surface free energy by orientating the surface into the non-polar region of the polymer [67].

According to the adsorption theory of adhesion, the interatomic and intermolecular interactions between adhesive and substrate are responsible for adhesive forces. These interactions are classified into primary (chemical bonding) and secondary forces (physical interactions, i.e. hydrogen bonding). The primary bonds are the strongest with energies in the range of 1000-100 kJ/mol as compared with 40-20 kJ/mol of secondary

forces. In case of urethane adhesives bonded to active hydrogen containing substrates, a primary bond is believed to exist [55].

Awaja et al. discusses multiple research groups in his review article [48]. One being Feinerman et al. who suggested that there are three zones for liquids interacting with polymers and that the surface tension of the solid is a function of the surface tension of the liquid [68]. He further postulated that;

- Zone 1 is the unperturbed zone; this indicates that the surface tension of a polymer is independent of the surface tension of the wetting liquid.
- Zone 2 is referred to as the additional polarization zone, here polymer surface tension is higher than in the unperturbed system.
- Zone 3 is termed the depolarization zone, where polymer surface tension is lower than the unperturbed zone.
- Zones 2 & 3 hold a linear dependence between the surface tension of the polymer and the surface tension of the liquid.

3.3 Matrix Carrier characterization

In Chapter IV of this work, two hot melt extrusion matrix carriers were used and rheologically investigated. The first compound in use was Soluplus® from BASF pharma chemicals Inc. The information and data for the polymer Soluplus® was taken from BASF Solubilizer Compendium report [53]. The second compound was calcium stearate. Information and background was taken from the USDA National Organic Program from UC SAREP [54].

3.3.1 Soluplus®

The co-polymer Soluplus® was especially developed as an innovative excipient for HME purposes as it enables new levels of solubility and bioavailability for poorly soluble active ingredients. On top of that, it features a low glass transition temperature T_g and high API stability. Unique in many ways, due to its remarkable properties for extrusion and excellent flowability, it displays superior performance in forming solid solutions. Those attributes make Soluplus® highly interesting for modern day drug delivery systems as it delivers the active pharmaceutical ingredient (API) in a dissolved state, resulting in improved bioavailability once in the body.

3.3.1.1 Composition

"Soluplus® is a polymeric solubilizer with an amphiphilic chemical structure, which was particularly developed for solid solutions." The biofunctional character enables Soluplus® to act as a matrix polymer for solid solutions on the one hand, while being capable of solubilizing poorly soluble drugs in aqueous media on the other hand.

Its chemical properties consist of a polyvinyl caprolactam – polyvinyl acetate – polyethylene glycol graft copolymer (13& PEG 6000/ 57% vinyl caprolactam/ 30% vinyl acetate). One or two side chains consisting of vinyl acetate randomly copolymerized with vinyl caprolactam, support the PEG 6000 backbone as visualized in figure 20.

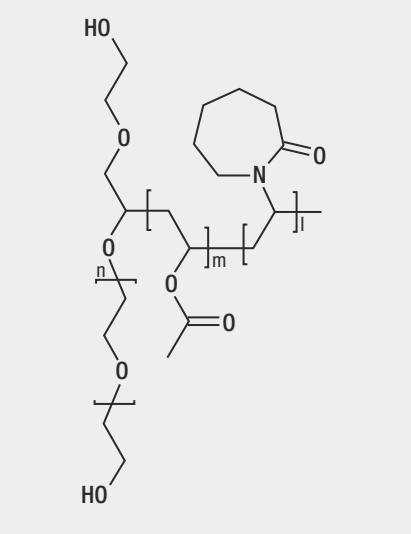

Figure 20: Chemical structure of Soluplus [71]

3.3.1.2 Properties

Visually, it consists of white slightly yellowish granules with a faint characteristic odor and practically no taste. The granules are spherically shaped and have a mean particles size of approximately 340 μm. Its free flowing features ensure proper feeding of extruder during processing.

It's molecular weight has a an average value of 118,000g/mol, which was determined by BASF using gel permeation chromatography. Since it was primarily developed for solid solutions, i.e. by means of hot-melt extrusion, "the glass transition temperature of the polymer was adjusted to approximately 70°C in order to enable extrudability at lower temperatures compared to already known polymers." Nevertheless, the temperature is still of a high enough level to ensure sufficient rigidness for proper storage stability of the final solid solution.

Having an amphiphilic structure, Soluplus® also has a detectable critical micelle concentration (CMC = 7.6 mg/L), which is much lower than can be found with classical low-molecular weight surfactants. CMC is a measure of surfactant efficiency. A lower CMC indicates less surfactant is needed to saturate interfaces and form micelles. Typical CMC values are less than 1% by weight [1].

3.3.2 Calcium Stearate

Calcium stearate is a non-toxic, white powdery substance. It is a calcium salt derived from stearic acid and is widely used in cosmetics, plastics, and pharmaceuticals as either a plasticizer, stabilizer, solid-phase lubricant that reduces friction between particles and surfactant. Calcium stearate is a substance that the U.S. Food and Drug Administration has generally recognized as safe when used as a food additive. However, it is important for our experimental purposes to notice, that calcium stearate is not a polymer.

3.3.2.1 Properties

"Calcium stearate is a metallic, water soluble stearate." It is a compound of Calcium with a mixture of solid organic acids obtained from edible sources, and consists primarily of variable proportions of calcium stearate and calcium palmitate. "It occurs as a fine, white to yellowish white, bulky powder having a slight, characteristic fatty odor."

3.3.2.2 Production

To produce Calcium stearate, calcium chloride, sodium stearate, and other salts of mixed fatty acids react in an aqueous solution. Consequently, the precipitate is isolated.

3.3.2.3 Applications

Its high versatility is accounted to its extremely low solubility. Calcium stearate can be used as an emulsifier, flavoring agent, anti-dusting agent, stabilizer, release agent or thickening agent. Other uses include water proofing, as a releasing agent for plastic molding powders, as a stabilizer for polyvinyl chloride resins, lubricant, and as a conditioning agent in various pharmaceutical products.

Chapter IV

4. Rheology and Adhesion of Pharmaceutical Polymers

4.1 Introduction

This Chapter covers, to a great extend the device that has been used for rheological investigations regarding two hot melt extrusion matrix carriers at the Research Center for Pharmaceutical Engineering.

4.2 Apparatus

For all measurements performed, an Anton Paar MCR301 Rheometer, fully fitted with an electric temperature controlled chamber (P-EDT400+H-EDT400) had been used. This device allows rotation tests as well as oscillation tests at increased temperature levels. Rheological data of Soluplus® provided by BASF has been measured by a plate-plate system. In contrast to the latter, the cone-plate system provides the advantage of homogeneous shear conditions in the whole sample.

Figure 21: Anton Paar Ind. Rheometer MCR301. [72]

4.3 Measurement Principle - Rheology

During the investigation, the rheological properties, of Soluplus® and calcium stearate had been thoroughly analyzed. Amplitude Sweeps, Temperature Sweeps and Frequency sweeps had been performed, the theory was explained earlier in Chapter 3. Now emphasis is laid on the experimental results, the data achieved and the consequently proceeded data analysis. The adhesion test will be explained later in this chapter.

4.3.1 Sample preparation

A rotational rheometer requires a uniform sample with a defined volume. It should be homogenous within the whole sample and centered spread on the ground plate of the measuring device.

The first material for investigation is Soluplus® powder provided by BASF. According to the compound analysis the material features a porosity of approximately 50%. Hence, when heated and brought above the glass-transition temperature, a non-uniform molten bulk with air bubbles on its surface area can be observed. To prevent this from happening and to create a uniform sample preparation the powder is compacted into a tablet, roughly 8 mm in diameter and approximately 1.65 mm in height. This procedure predefines the shape, the mass of the sample, and reduces the porosity from 50% of the bulk material to about 15 % of the tablet. Thus, less air is entrapped within the sample and sample volume can be set by the tablet mass and known density. This step solved the problem for uniform sample preparation but not the entrapped air within the sample. The entrapped air biases the results in two possible ways; first, it enlarges the sample volume and leads to an overfilling of the measurement gap. Second, the bubbles distort the laminar flow pattern in the measurement gap.

To eliminate air bubbles that are consequently formed when the material is heated due to remaining pores, the tablet is molten in a vacuum oven. A single tablet is heated under 200 mbar and 180°C for ten minutes. When preparing samples for the larger Plate-Plate 25 mm system, 2 tablets lying on top of each other, are molten under 200 mbar for about 70 minutes.

This procedure removes all the remaining air from the tablets and ensures testing with lower susceptibility to errors. In contrast, the old sample preparation only consisted of centrally spreading the dry sample powder on the heating surface without any previous treatment. The sample preparation is illustrated in figure 22.

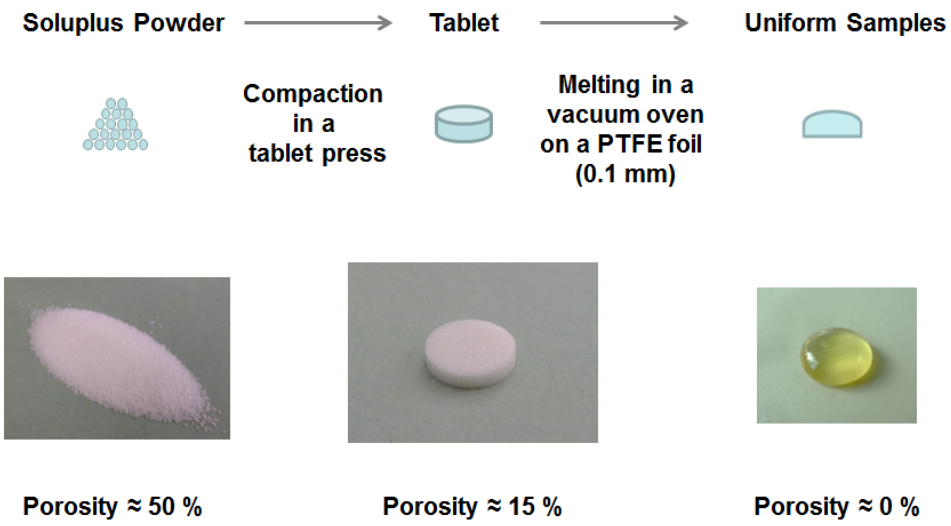

Figure 22: Illustration of the developed sample preparation method for Soluplus® [3]

Due to its great flow properties Soluplus® was the ideal material for compaction. The tablets were compacted with a Stylcam 200R compaction simulator (Medelpharm, France) in an automated process. On the other hand, the second matrix carrier, calcium stearate does not feature such attributes.

Therefore, automatic compaction was not possible. Also when molten in the vacuum oven at high temperatures, the material didn't melt but showed dissolving characteristics. Furthermore, something what was probably a nonenzymatic browning effect, such as the Maillard reaction, caused carbonization on the top layers of the substance.

In the end calcium stearate was compacted manually to tablets with the help of a Vacuum-press. Nevertheless, samples in tablet formulation were still more then frail and volatile to break apart. Special care had to be taken.

4.3.1 Experimental Procedure

Followed by the successful sample preparation we now have to ensure that the pre-molten tablet can be placed with high enough precision onto the very center of the Rheometer's heating plate. Placing the tablet a few millimeters off-center would result in the molten polymer not properly covering the sensor surface of the measuring system, hence leading to distorted and non-reproducible results.

For this purpose a special centering device had been created at the Research Center for Pharmaceutical Engineering. Figure 22 illustrates the scheme of the centering device. This device fits smoothly onto the Rheometer's heating plate (4), without leaving a gap for possible errors and consists of a punch (1), an adapter (2) and centering device (3). Different denominations of the adapter are available for different sample sizes. The punch is used for powder compaction, if applicable.

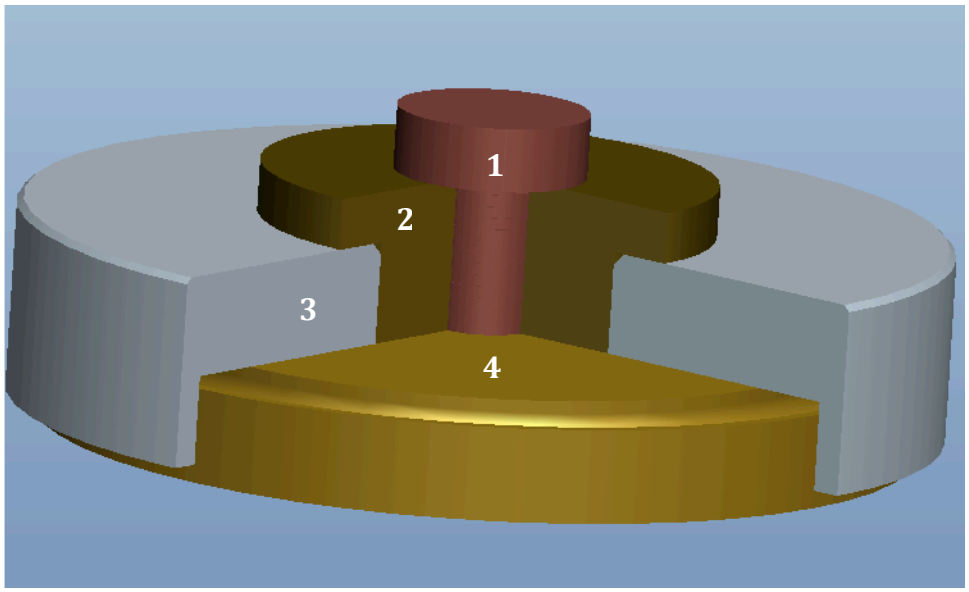

Figure 23: Centering device developed at RCPE, Graz

In order to select the correct measuring system for the Rheological tests, comparison of the reproducibility of previous experiments as well as feasibility and constraints of the measurement range were accounted for. Each of the systems used in this project are illustrated in figure 24;

Measuring Head	Gap [mm]	Shear Rate [1/s]	Shear Stress [Pa]
PP 8	0.25	4.996	2.025*10E6
	0.50	2,498.19	2.025*10E6
	1.00	1249.1	2.025*10E6
PP 25	0.25	15,689.4	65,422
	0.50	7,844.68	65,422
	1.00	3,922.34	65,422
CP 25	0.047	18,104.6	48,941.5

Figure 24: Limitations of the measuring system

The measuring head that was chosen for these investigations is a cone-plate system, having 25 mm cone diameter and 1° angle.

4.3.3. Data Analysis and Discussion

Measurements were performed with the Anton Paar MCR 301 Rheometer device, which has been previously described. Plate-plate and cone-plate systems had been used in denominations of 25 mm and 8 mm measuring head surfaces, respectively.

4.3.3.1 Errors and tainted results

Now before emphasizing on the actual data that we achieved and measured throughout this project, it is very important to understand that the rheological measurements performed are highly susceptible to errors. To prevent these from happening and creating distorted results one has to fundamentally understand their nature and origins.

In the heading for ‘sample preparation’ a small insight was already given for various errors that can occur associated with the sample itself.

One paramount aspect is to comply with weight and size regulations for the sample to prevent over- or under filling. In the case of over filling the gap between measuring head and the heating plate, the molten polymer could overlap, attach itself onto the side or top of the plate measuring system and cause distortions. While the effect of under filling might result in the measuring head not being able to properly compress the sample.

The same effect as observed with over and / or under filling might be caused by the sample not being correctly placed onto the very center of the Rheometer's heating plate. On one side the molten substance might overlap with the sensor, while on the other side no substance would be analyzed by the measuring system at all, due to the precise geometrics that adhere between sample and system. Possible errors are illustrated in Figure 25 below;

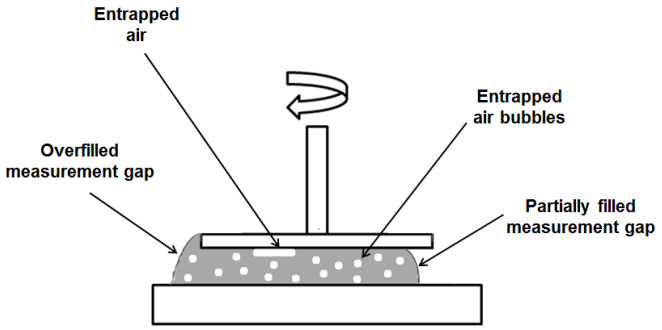

Figure 25: Illustration of possible measurement errors [3]

4.3.3.1 Amplitude Sweep – Soluplus®

Figure 26 shows three experiments for an amplitude sweep for Soluplus® with a cone-plate 25 mm system measured at 170°C and a constant gap of 0.047mm respectively. The angular frequency was held at 100 rad/s.

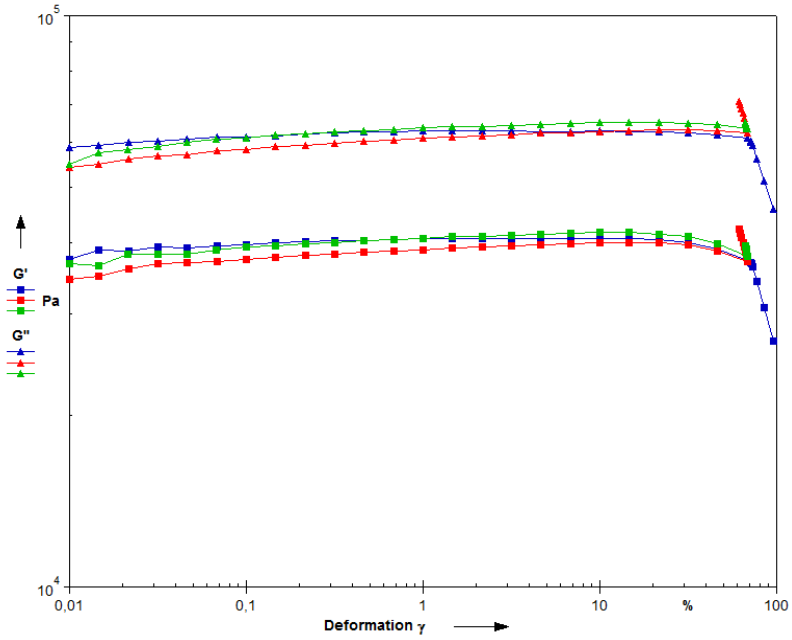

Figure 26: Amplitude Sweep CP25 170 Soluplus®

During amplitude sweep the amplitude of the deformation is increased while the frequency is kept constant. For the analysis the storage modulus G' and the loss modulus G'' are plotted against the deformation. The illustration depicts that at low deformation G’ and G” are more or less constant. The measuring device has, most likely caused small irregularities that occurred at low deformation. Towards the end, as soon as the moduli start to decrease, the structure is disrupted. This disruption is associated with the end of the LVE-region. The ratio of the two moduli gives information about the characteristics of the sample [6].

If the storage modulus G’ is larger than the loss modulus G” the sample behaves more like a viscoelastic solid, but in the case of Soluplus® at 170°C.

G”proves to be significantly larger then G’, which demonstrates the properties of a viscoelastic fluid. Nevertheless, in the high deformation area the maximum capacity for the measurement had been reached by the rheometer’s limitations as no further measurements can be produced in ‘Direct strain option’ mode. This results in the data distortion that can be observed in all data curves at deformation above 70%. The effect is most likely caused by the deflection of 1000% at 100 rad/sec. If the frequency is lowered to about 10 rad/sec, which is aligned to a standardized deflection of 100%, this effect could be bypassed in further experiments.

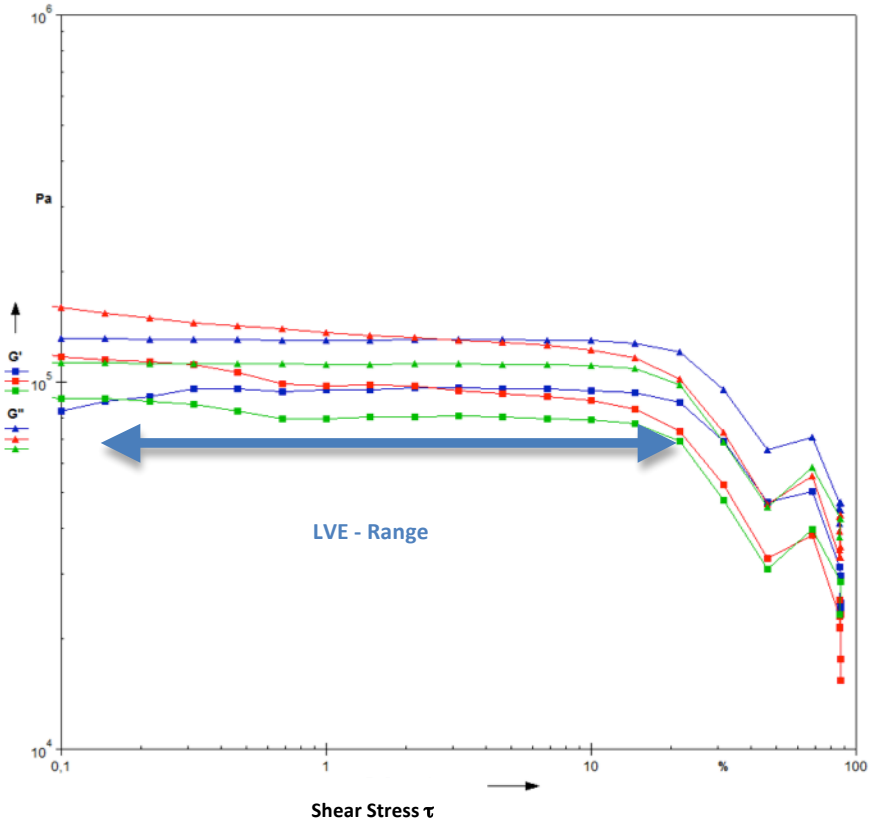

Figure 27: Amplitude Sweep PP8 170 Soluplus•

In addition three runs for an amplitude sweep had been performed with a plate-plate 8mm system at 170°C and an angular frequency of 100 rad/s; In contraire to the CP-

system a gap of 1 mm had been chosen for the PP measurements; The tendencies between storage and loss moduli are not as apparent as with the CP 25 system. This can be seen in the illustration of figure 27.

Especially at low deformation the PP8 is showing irregularities with high variations in the data. Towards the end of the LVE-region the decrease commences steady and prolongs the distortions recorded at the low range. Similar to the CP25 system, this can be attributed to the same effect and could be foregone by lowering the amplitude.

4.3.3.2 Frequency Sweep – Soluplus®

Figure 28 depicts three assays for a frequency sweep for Soluplus® with a cone-plate 25mm system measured at 170°C and a constant gap of 0.047mm respectively. The amplitude was held at 0.1%.

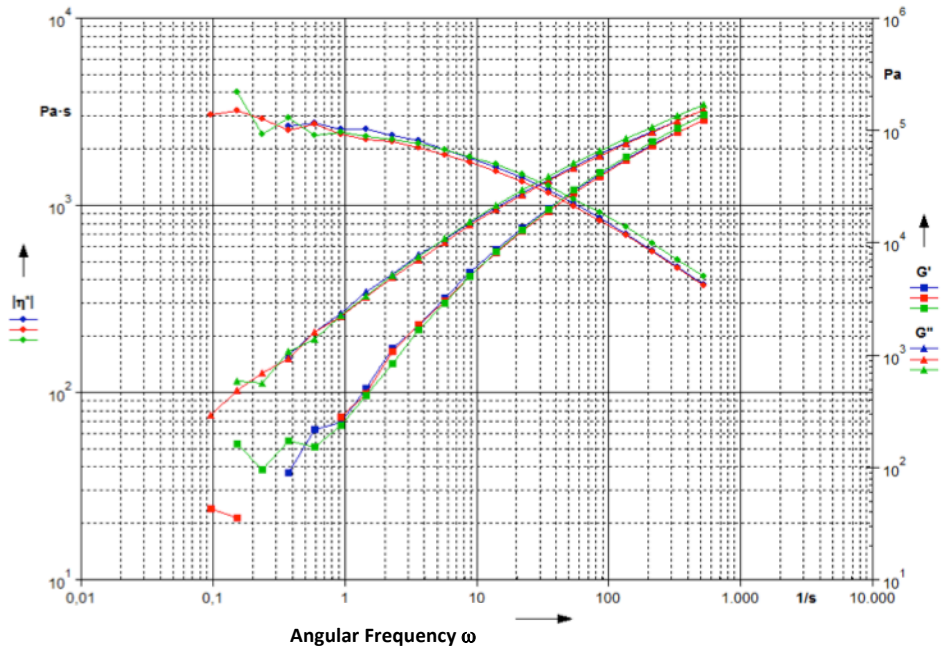

Figure 28: Frequency Sweep CP25 170 Soluplus®

During the frequency sweep the frequency is varied while the amplitude of the deformation is kept constant. For data analysis the storage and the loss modulus are plotted against the frequency, as can be seen in figure 28. The frequency sweep is important for polymer melts [10]. All experiments were held within the LVE range. The data shows good reproducibility with an angular frequency set from 0.1 to a maximum of 526 rad/s.

However, when the measurement reaches the lower resolution limit, one can clearly observe intemperance of the curves. This could be associated with measurement irregularities or actual distortions of the measurement system. In this test the loss modulus was always higher than the storage modulus.

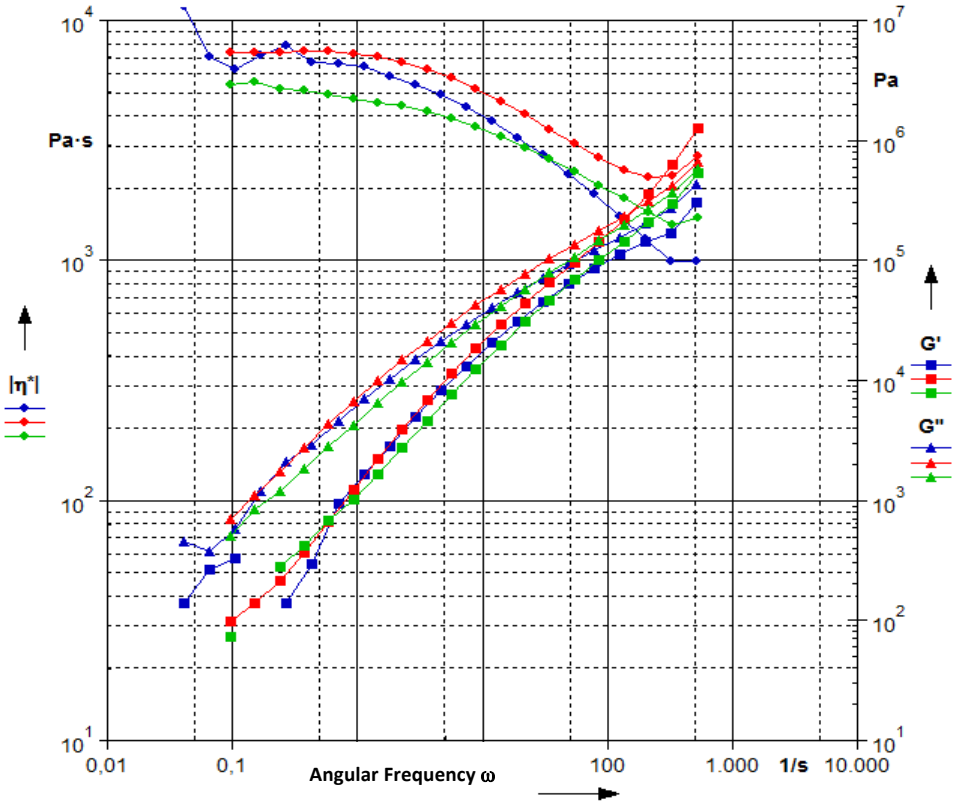

Figure 29: Frequency Sweep PP8 170 Soluplus®

Figure 29 compares three frequency sweeps for Soluplus® with a plate-plate 8 mm testing system at 170°C and a measurement gap of 1 mm; again the angular frequency

was set from 0.1 to a maximum of 526 rad/sec and the amplitude kept at 0.1% Unlike the data achieved for the CP25 system, the viscosity curve shows rather weak reproducibility, as well as for the repeated intemperance towards the end of the measurement. One has to also acknowledge that for the frequency sweep with the PP8 measuring system, the 'old' sample preparation had been used. Hence when comparing the two assays for PP8 and CP25 (old vs. new) one can observe a vast difference in the quality of the results.

4.3.3.3 Temperature Sweep – Soluplus®

Figure 30 shows a temperature Sweep for Soluplus® with a cone-plate 25 mm system measured starting at 220°C and a constant gap of 0.047mm respectively. The angular frequency was set to 10 rad/sec and the amplitude kept at 0.1%.

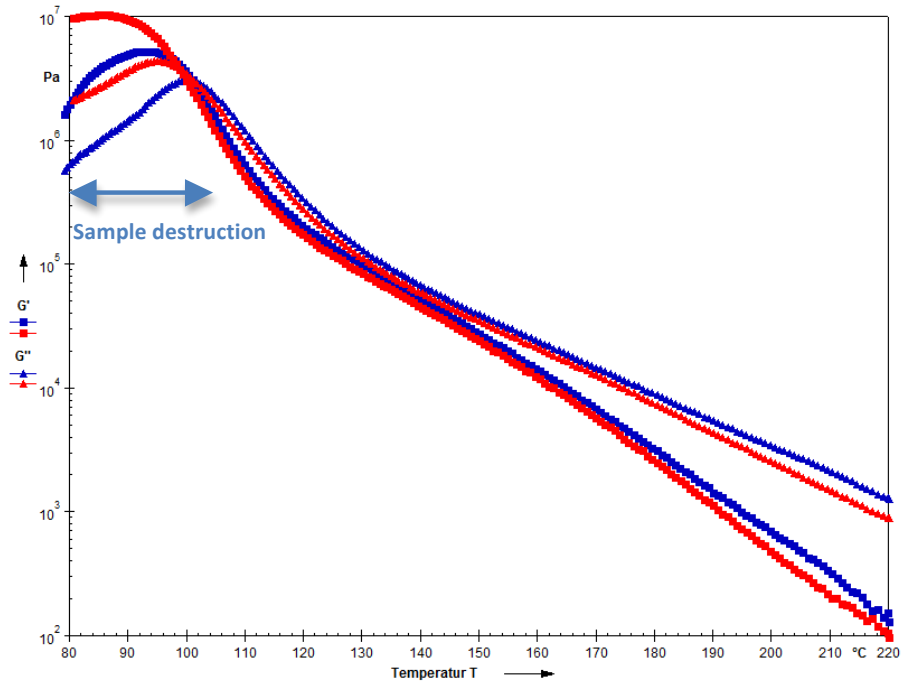

Figure 30: Temperature Sweep CP 25 220 Soluplus®

The TS assay shows two runs with good reproducibility in its data for temperatures of above 100°C. Evidently the data shows some deviations below the 100°C benchmark as

both, storage and loss modulus heavily decrease. Torque limitations from the Rheometer restricted the emasurements from reaching temperature values around the lower limit set at 60°C. The intersection point between storage and loss modulus, observed at around 105°C refers to the glass transition of Soluplus®. The glass transition temperature is described by the intersection of the loss and storage modulus. It is assumed that the viscoelastic region is abandoned at temperatures below 105°C, which result in product destruction of the polymer. However, if the amplitude is lowered, this effect could be bypassed. This effect most likely is to take place outside of the LVE range. Since Soluplus® has a glass transition temperature of ΔT = 70 - 80°C no compliance with literature and experimental data could be found.

Figure 31 illustrates another Temperature Sweep for Soluplus® performed with a plate-plate 8 mm system at a starting temperature of 220°C. The measuring gap was set at 1mm.

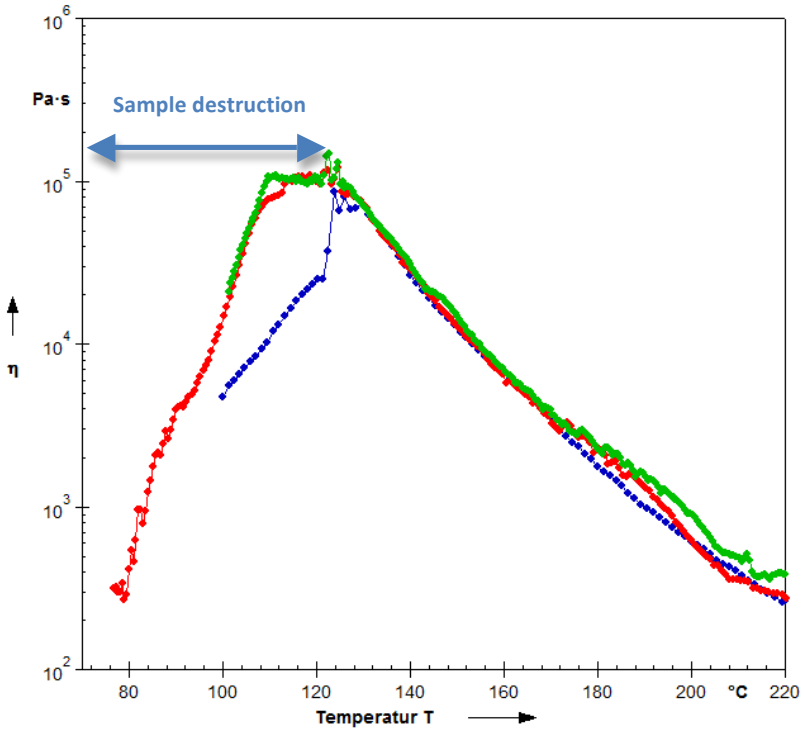

Figure 31: Temperature Sweep PP8 220 Soluplus•

In this test comparison the difference between the old and 'new' sample preparation is apparent. The green and red data curves represent the aforementioned sample

preparation in form of tablets. The blue line is Soluplus® powder arbitrarily spread onto the Rheometer's heating plate. The 'old' variation cannot produce constant data nor can it perform a steady data acquisition below 130°C.

4.3.3.4 Amplitude Sweep – Calcium Stearate

Figure 32 shows an amplitude sweep for calcium stearate with a cone-plate 25 mm system measured at 200°C and a gap of 0.047mm respectively. The angular frequency was held at 100 rad/s. Two test runs are compared.

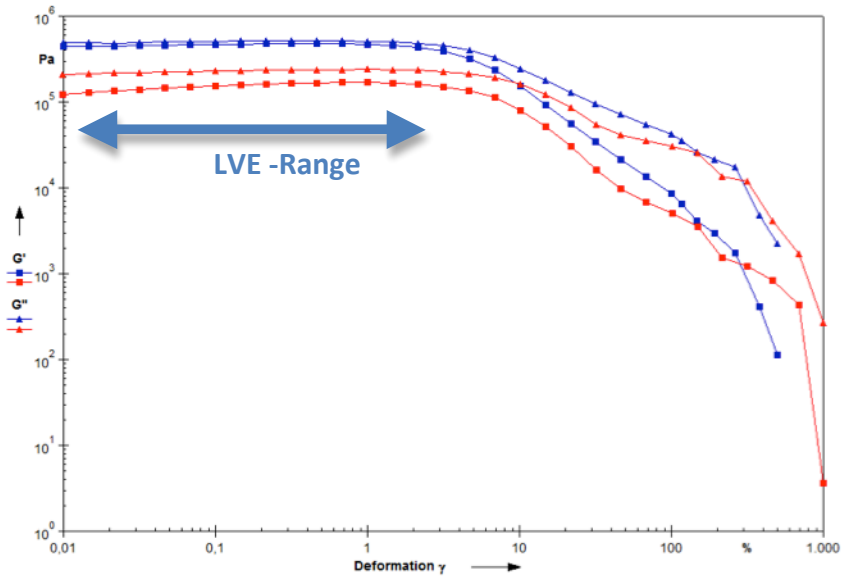

Figure 32: Amplitude Sweep CP25 200 Ca St

For the interpretation of the Rheogram for calcium stearate a different scaling was used as for Soluplus®. This is due to the fact that the data recorded for the amplitude sweep has much greater intemperance after leaving the LVE-Range past 5% of deformation. This can probably be attributed to the difficult sample preparation involved with experiments conducted with calcium stearate.

4.3.3.5 Frequency Sweep – Calcium Stearate

Figure 33 shows a frequency sweep for calcium stearate with a cone-plate 25mm system measured at 130 degrees Celsius and a constant gap of 0.047mm respectively. Again, two experimental procedures are compared. The amplitude was kept at 0.1%.

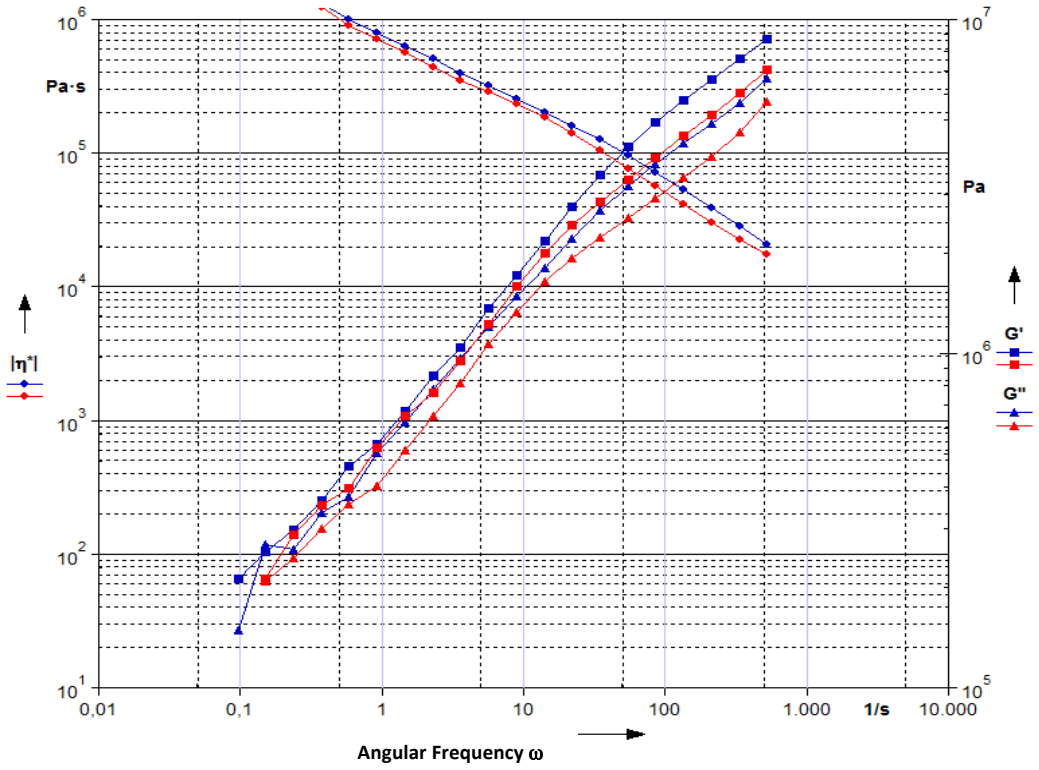

Figure 33: Frequency Sweep CP25 130 Ca St

The data recorded for the assay shows decent alignment towards the lower limit of the frequency with some minor discrepancies in the loss modulus G". However, we were not able to reproduce the reproducibility seen at the Soluplus® frequency test. Especially, if one observes the higher regions of the measurement resolution. The angular frequency was held from 0.1 to a maximum of 526 rad/s. It is assumed that the rheogram depicts a viscosity curve according to a Power Law.

4.3.3.6 Temperature Sweep – Calcium Stearate

Figure 34 shows two measurements for a temperature sweep for calcium stearate with a cone-plate 25 mm system measured starting at 220°C and a constant gap of 0.047mm respectively. The angular frequency was set to 10 rad/sec and the amplitude kept at 0.1%.

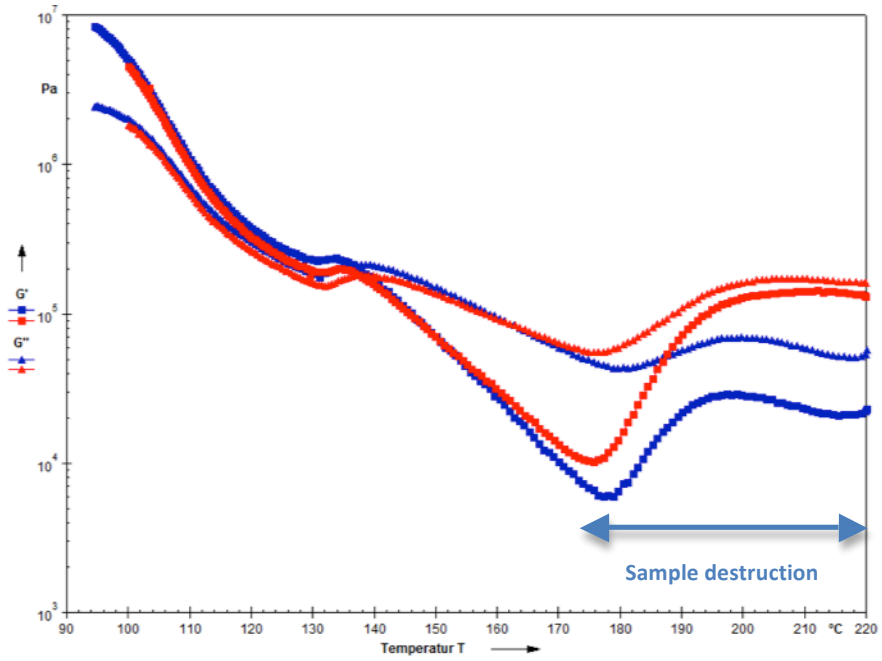

Figure 34: Temperature Sweep CP25 220 Ca St

In this Temperature Sweep for calcium stearate the data illustrates very good reproducibility starting with temperatures below 170°. Unlike the temperature Sweep for Soluplus®, calcium stearate does not show strong alignment in the region between 170° and the starting point of 220°. This effect might be due to the very unpredictable stability of calcium stearate in higher temperature regions. The point of intersection, observed at around 140° usually indicates the melting point of the substance or the glass transition.

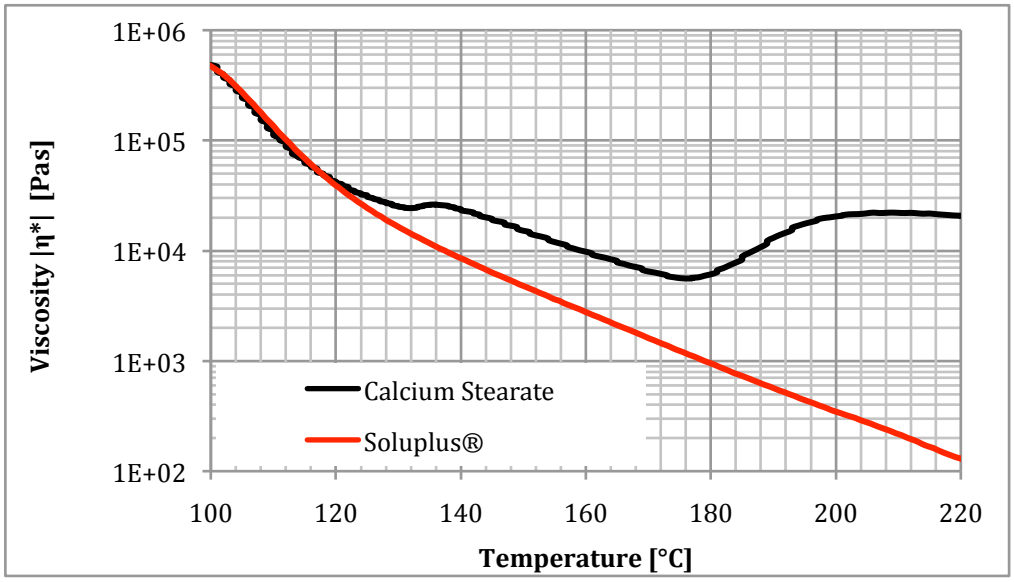

Figure 35: Complex viscosity comparison of Soluplus® and Calcium Stearate

In figures 35 and 36 the comparison between calcium stearate and Soluplus® is depicted. Soluplus® shows a simple thermo-rheological behavior, which can be mathematically described through the time-temperature-shift, whereas calcium stearate is far more complex and there no approximated mathematical model available.

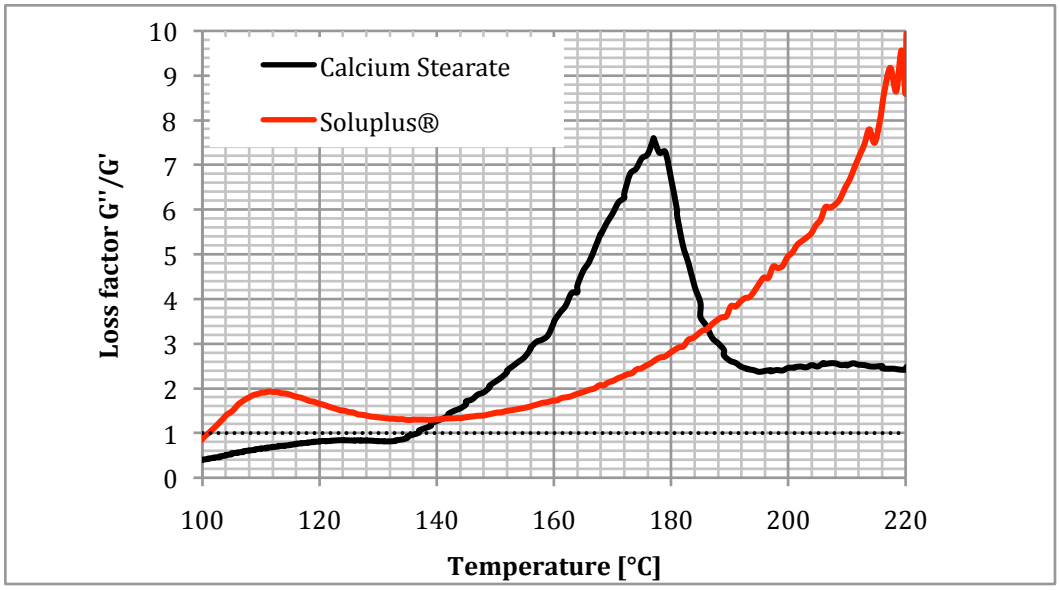

Figure 36: Loss factor comparison between Soluplus® and Calcium Stearate

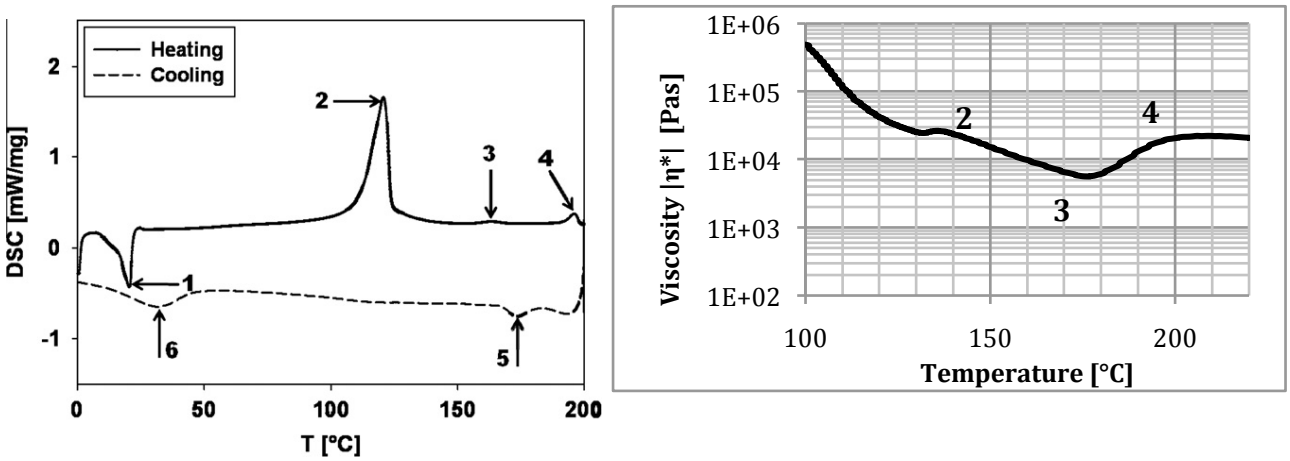

Figure 37: left: DSC thermogram of the first heating and cooling cycle of Calcium Stearate [73]; right: Rheologial Temperature Sweep of calcium stearate

Figure 37 shows a thermogram of calcium stearate and describes its regions as follows [73]:

1. Exothermic peak at 20.3°C (phase transition)
2. Endothermic peak at 120.7°C (structural rearrangement, i.e. transition of the crystalline state into the liquid crystalline state)
3. Endothermic peak at 163.9°C (smectic mesophase becomes nematic)
4. Endothermic peak 196.3°C (transition of the nematic state into liquid state)
5. Exothermic cooling peak at 173.4°C
6. Exothermic cooling peak at 37°C

4.4 Measurement Principle – Adhesion

4.4.1 Experimental Procedure

For analyzing purposes the preparatory operation of the adhesion test in comparison to the oscillatory tests, stays much the same. The same sample preparation had been used as discussed earlier in this chapter. Again the Polymer is placed with the help of our developed centering device onto the Rheometer's heating plate. Both Soluplus® and calcium stearate were analyzed at different temperature levels. Adhesion tests were performed with a plate-plate 25 mm and a plate-plate 8 mm testing system, respectively. The theoretical principles of the tack test procedure are illustrated in figure 38.

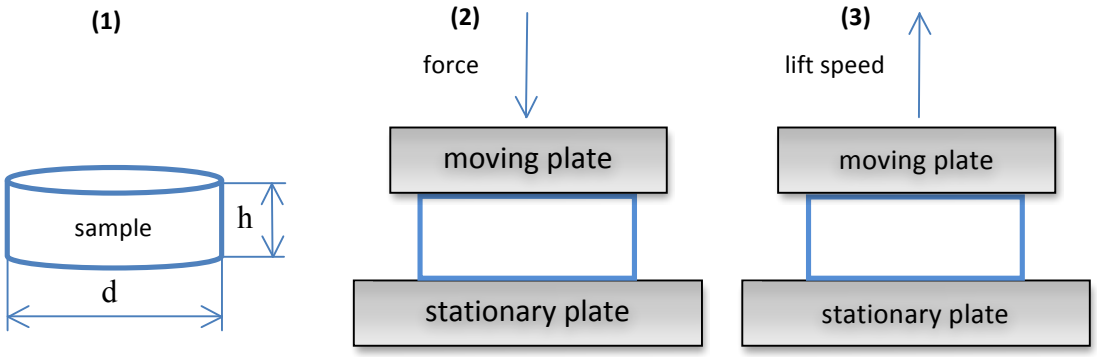

Figure 38: Tack Test principles

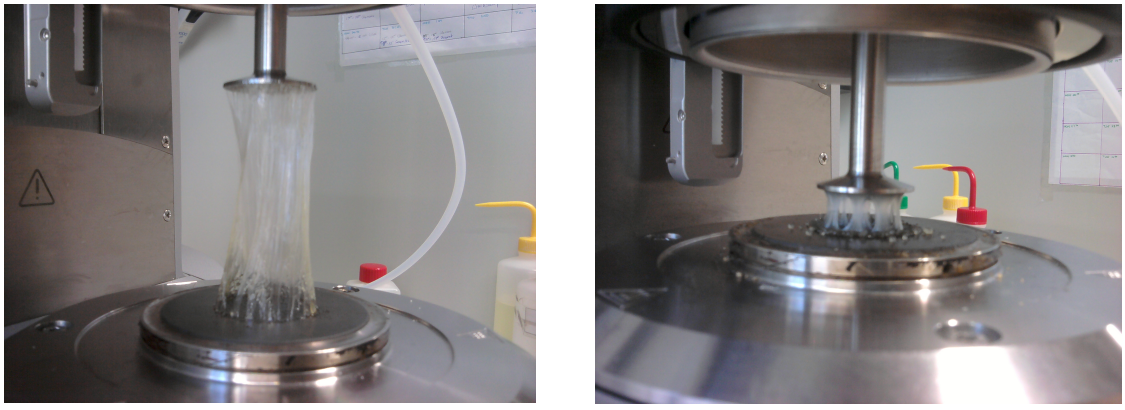

Figure 39: Tack Test snapshots Soluplus•

Figure 39 illustrates two snapshots taken during adhesion experiments with Soluplus®. This phenomenon, as seen in the pictures is described by A. Zosel as fibril growth [74]. In his article he further manifests that the formation and growth of fibrils during the debonding is crucial to the peel strength.

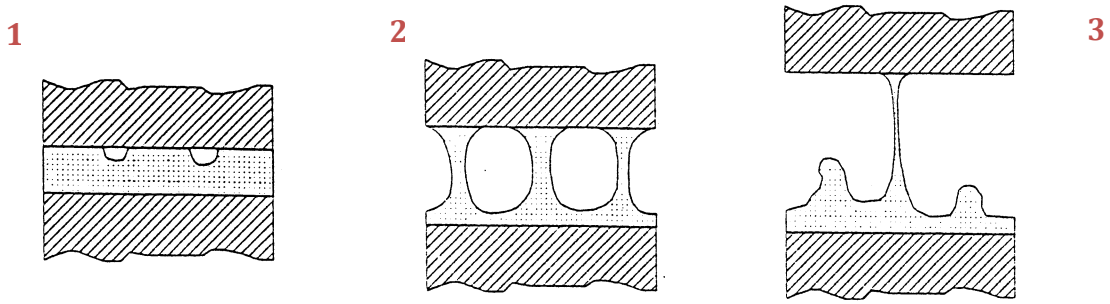

Figure 40: Fibrilation scheme [74]

Fibrillation is schematized as a three-step process of the formation of fibrils, their deformation and their debonding, which is illustrated in figure 40. The process is explained in the schematic diagram as follows: (1) cavitation; (2) fibril growth; (3) separation.

4.4.2 Data Analysis and Discussion

Data was best recorded at higher temperatures. For Soluplus® 170°C was the norm, as for calcium stearate 200°C was used to melt the substance.

Initially a gap of 1 mm was sought after for all measurements with the plate-plate 25 mm system, but as the Rheometer reached its limitations and showed vastly irregular data, a compromise was made to only measure calcium stearate with the PP8 system. Nevertheless, the plate-plate 25 mm system used a gap set at 1 mm, for experiments conducted with Soluplus®. The following specifications were used in tack tests for both, Soluplus® and calcium stearate;

Tack Test Specifications		
Waiting Position	Profile	constant
	Measuring point	0.1 sec.
	Segments	10 sec.
Force	Normal Force	0 N
Peeling Stage	Profile	Ramp log
	Starting Value	-0.02 mm/s
	Ending Value	-0.05 mm/s

Figure 41: Tack Test specifications

4.4.2.1 Tack test – Soluplus®

Figure 42 depicts two measurements for a Tack test for Soluplus® performed with a plate-plate 25 mm measuring system at 170°C, compared to two runs of a plate-plate 8mm system with the same specifications.

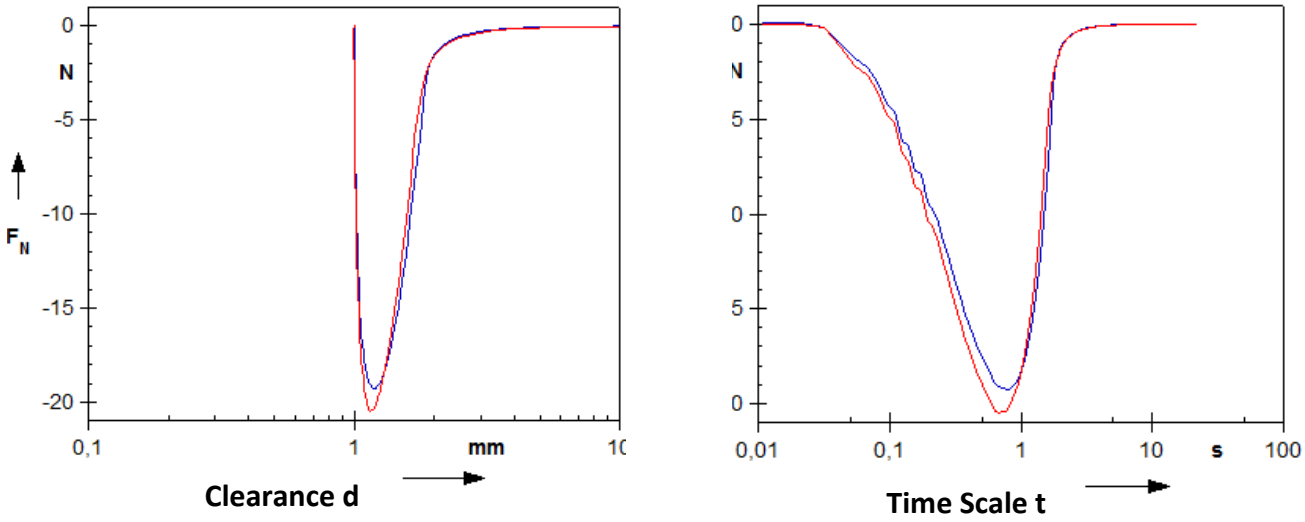

Figure 42: Tack Test PP25

Figure 42 shows the tack profile of the experiment. Tack strength of approximately 20 N was observed during the test, as well as a comparably high tack energy, which is illustrated through the width of the tack peak. During the measurement process the residence time of the measuring head on molten polymer surface was recorded at a maximum of 10 seconds.

4.4.2.2 Tack test – Calcium Stearate

In the first Tack Test measurements for calcium stearate the PP25 system was used. However, due to the fact that process limitations were reached with the Rheometer, the decision was made to measure with a PP8 system instead. Figure 43 clearly shows the limitations reached and the high irregularities recorded.

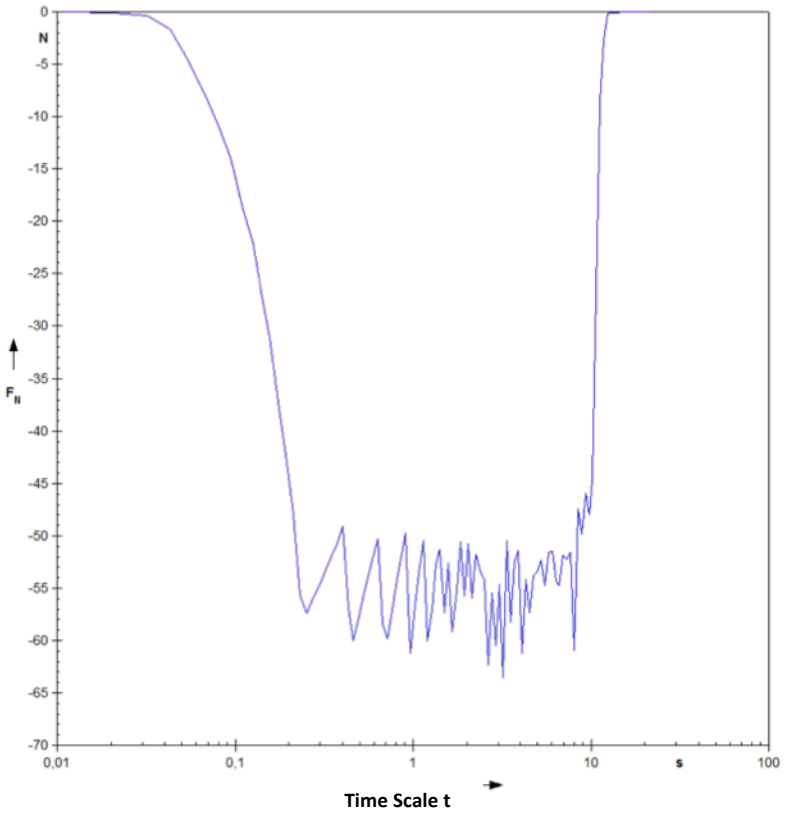

Figure 43: Tack Test PP25 Calcium Stearate

A table will provide insight information on why a PP8 system was chosen in favor over a PP25 measuring head. Where Sigma gives the maximum tensile strain, which equals the force in respect of the area. Maximum 'normal force' according to the MCR301 data sheet is valued at -65.4 N respectively.

d [mm]	A [mm^2]	A(25)/A(d)	Sigma(max) [N/mm^2]
4	12.6	39.1	-5.20
8	50.3	9.8	-1.30
15	176.7	2.8	-0.37
25	490.9	1.0	-0.13

Figure 44: Measuring system profiles

Figure 45 depicts a tack test for calcium stearate performed with a plate-plate 8 mm measuring system at 200°C. Due to measuring difficulties no experiments with a PP25 system were conducted. Two experimental measurements are illustrated.

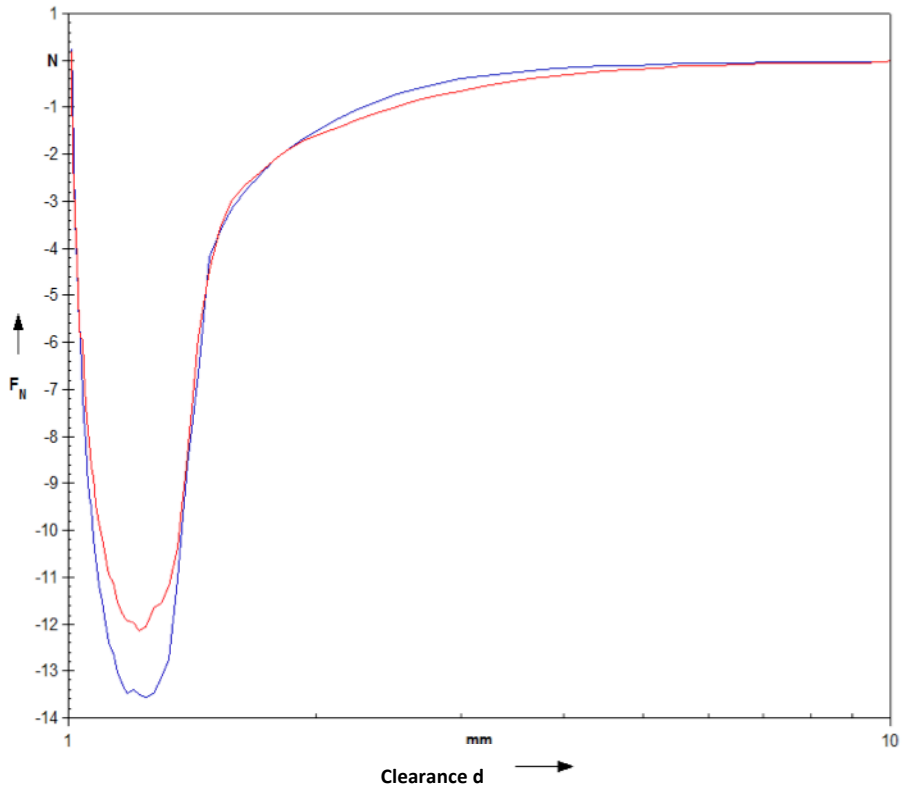

Figure 45: Tack Test PP8 Calcium Stearate

According to literature, calcium stearate generally shows non-tack properties. In industry it is commonly used as a lubricant. Contradictive is, that If compared to the adhesive force of Soluplus®, calcium stearate shows much higher tack strength, recorded at approximately 12 to 14 N with a PP8 system. Figure 45 also clearly indicates that the substance's tack energy is higher than that of the polymer Soluplus®, observed in the significantly wider peak width.

The following comparison should ratify the assumptions stated in this chapter. Figure 46 compares the results achieved for both carriers conducted with the PP8 measuring head.

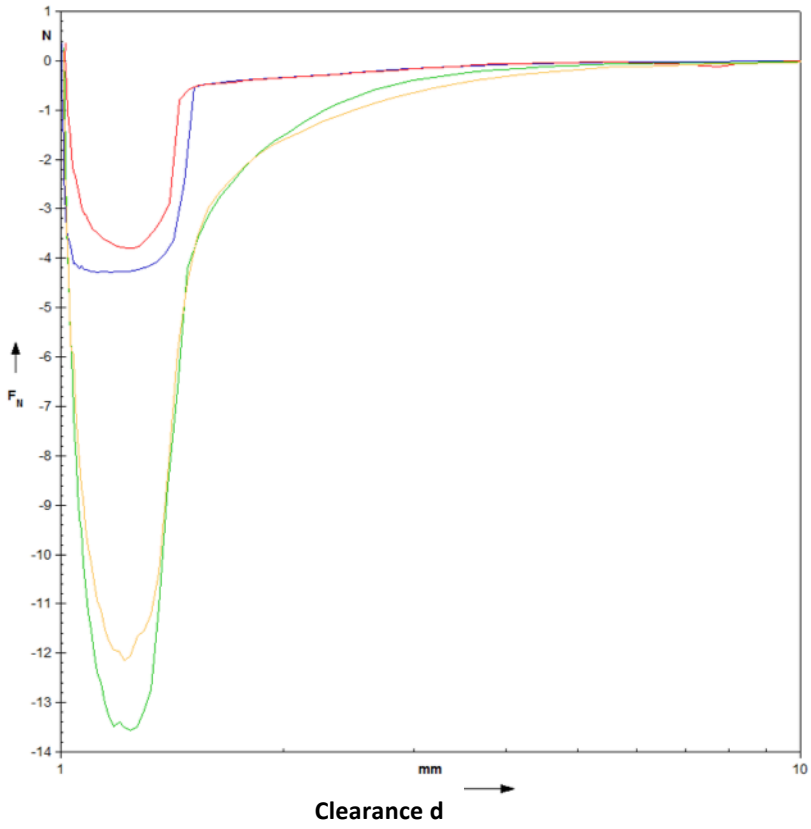

Figure 46: Comparison of PP8 for Soluplus® and Calcium Stearate

The figure clearly shows that Soluplus® (red and blue data curves) has limitations and actual problems to achieve a 'tack' or adhesion on calcium stearate with the PP8 measuring head. This might be due to the measuring head's smaller contact area. Based on theses measurements the decision was made that the plate-plate 25 mm system, is the measuring head of choice for Soluplus®. The results are highly contradictive to literature as it is assumed that Soluplus® should feature much higher tack strength than calcium stearate.

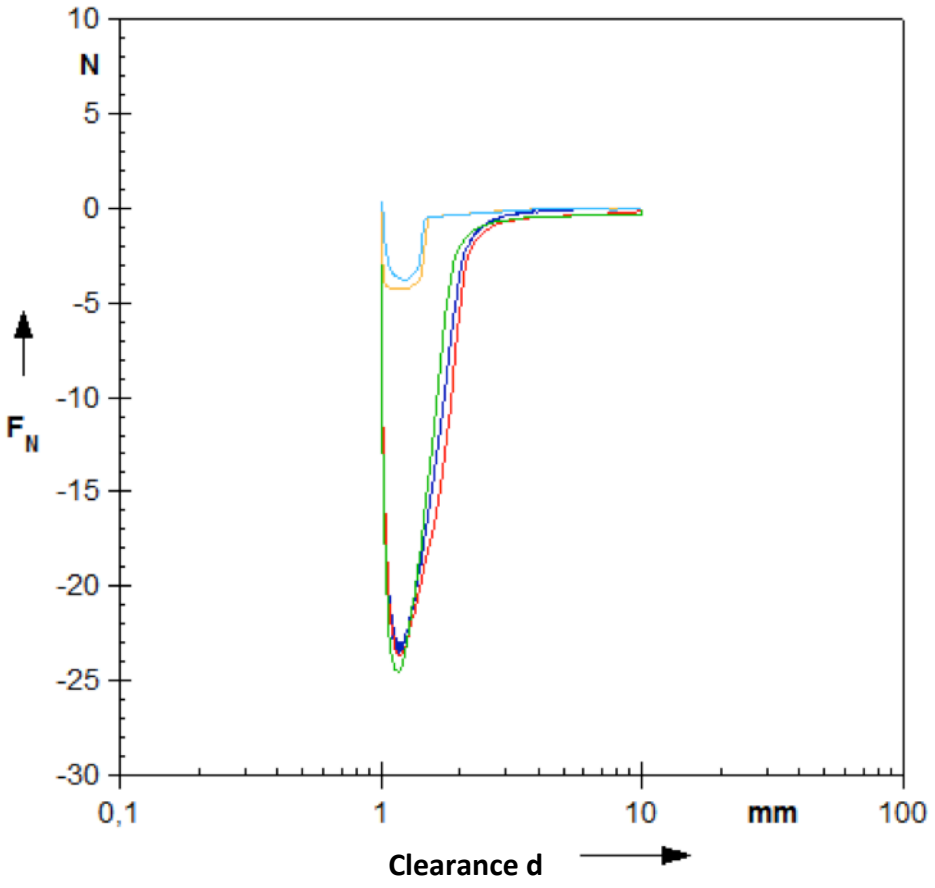

Figure 47: Comparison between PP8 and PP25 for Soluplus®

Figure 46 depicts a comparison between Soluplus® measured with both PP8 and PP25 measuring heads. Obviously the PP8 requires much less normal force than the PP25

system. This effect is explained by the difference in contact area between the two measuring heads.

The average peak value of PP25 data is 23 N and 4 N for the data peaks acquired with the PP8 system. The ratio of both means results in 5.8; which does not cohere with the previously calculated factor 10 for the PP8 measuring head (see figure 42). The distinction between the ratios could be explained by the partial similarity of the experiments. The measurement gap was not adjusted to compare geometric analogy; nevertheless further research should be conducted in this area to clarify the relation between geometry and normal force.

To summarize all results mentioned in regard of adhesion tests in this chapter, one can acknowledge that further research is needed to manifest proper lasting theories about tack characteristics. The experimental data for both, calcium stearate and Soluplus® were contradictive and did not correspond with literature. However, within our own limitations the data recorded showed mostly good reproducibility.

5 Summary and Conclusion

In Chapter I, the fundamental ideas of rheological research and its background directly related to the measurements in this thesis, have been explored and thoroughly explained. In Chapter II, theory, historic figures and experiments have been presented along with modern day applications that have been developed by scientists with great guile within the past decades. Emphasis was laid on procedures and techniques to determine rheological properties of polymers. While chapter III emphasized on the fundamental background of testing adhesiveness. Theoretical as well as mechanical principles were used to describe the phenomenon of adhesion. Chapter IV presents the experimental data recorded along with elemental analysis of the data achieved from testing procedures for both rheological properties and adhesiveness.

Experiments for both rheological properties and adhesiveness of the hot melt extrusion matrix carriers Soluplus® and calcium stearate have been performed. Substance characteristics had been analyzed by conducting Frequency Sweeps, Amplitude Sweeps and Temperature Sweeps, respectively. In a separate testing procedure, adhesive properties were analyzed by Tack tests.

The vast knowledge gained through the testing procedures give a comprehensive insight into the behavior of the two hot melt extrusion matrix carriers. Uniform sample separation is a paramount aspect in recording clean and reproducible data values. Clean and tidy work in regard of sample contamination is very important. Possible impurifications on the measuring head should be avoided. For clear data interpretation, coherent scaling and validation of results as well as revision and literature comparison should be complied with.

Some testing procedures apply heavy stress onto the sample and the substance. Under certain circumstances, this may lead to product destruction, which would manipulate the recorded data and cause distortions and irregularities.

Overall, to minimize the possibility of product destruction during the experimental test, if LVE-range is abandoned, one can forego the following two procedures to prove that no destruction is prevalent:

- Measuring twice with the same sample, yielding the same data would eliminate the possibility of product destruction.
- A time sweep with a given frequency, amplitude and temperature at a pre defined time scale, would prove no product destruction has taken place, if both test runs show a close analogy

The difficulty in obtaining reliable experimental data accounts for the reputation of inconsistent results; associated with the tack properties of both calcium stearate and Soluplus®. The Tack tests performed show reproducible data for Soluplus® with the plate-plate 25 mm measuring head and for calcium stearate with the plate-plate 8 mm system. Nevertheless, the results obtained did not cohere with literature values and as discussed in the applicable chapter, were quite contradictive. Testing adhesiveness is a highly volatile and yet not fully understood area and requires more fundamental testing in the near future.

References:

[1] Manufacturing chemist; API dispersal through HME; ISP Pharmaceuticals, (2011)

[2] Jana S., Miloslava R.; Hote Melt Extrusion; Ceska Slov Farm. Vol.61 (3), 87-92, (2012)

[3] G. Koscher, A. Eitzlmeyer, D. Treffer, C. M. Smola, S. Windhab; Development of an Industrial HME Process for Pharmaceutical Pellet Production – Internal report; Research Center for Pharmaceutical Engineering GmbH, (2012)

[4] S. Radl, T. Tritthart, J.G. Khinast; A novel design for hot melt extrusion pelletizers; Chemical Engineering Science, Vol. 65, 1976-1988, (2010)

[5] T. Reintjes (editor); Solubility enhancement with BASF Pharma polymers; Solubilizer Compendium, BASF Pharma GmbH, (2008)

[6] Mezger T. G.; The Rheology Handbook, 2nd Edition; Vincentz Publishings (2006)

[7] Ebah, The Role of Rheology in Polymer Extrusion, taken from www.ebah.com.br

[8] Bird R. B., Stewart W. E., Lightfoot E. N.; Transport Phenomena, 2nd Edition, John Wiley & Sons, Inc. (2007)

[9] Green Book, 2nd ed.: IUPAC Quantities, Units and Symbols in Physical Chemistry. 2nd Edition, Blackwell Scientific Publications, Oxford (1993)

[10] J. Laeuger, M. Bernzen; Getting the zero shear viscosity of polymer melts with different rheological tests; Physica Messtechnik GmbH, Anton Paar, (2009)

[11] Morrison I.D., Ross S.; Colloidal Dispersions: Suspensions, Emulsions and Foams; Wiley Interscience Publishings (2002)

[12] Rheotec Germany; Introduction to Rheology, Basics, Rheo Tec Messtechnik GmBH, Ottendorf-Okrilla (2006)

[13] Somwangthanaroj A.; Rheology and Polymer Characterization; Chulalongkorn University, Bangkok, Thailand (2010)

[14] Metzner A. B., Reed J. C.; Flow of non-Newtonian Fluids- Correlation of the Laminar, Transition, and Turbulent-flow Regions; A.I.Ch.E. Journal, 434, (1955)

[15] Scott Blair, G. W., "Introduction to Industrial Rheology; J & A Churchil (1938)

[16] Reed, J. C., M.Ch.E. Thesis, University of Delaware (1954)

[17] R.P. Chhabra; Non-Newtonian Fluids: An Introduction, India Institute of Technology, Department of Chemical Engineering (2002)

[18] M.M. Cross; Rheology of Non-Newtonian Fluids: A new flow equation for pseudoplastic systems; Journal of Colloid Science, 20, 417-437 (1965)

[19] O. Reynolds; On the dilatancy of media composed of rigid particles in contact; Philos. Mag. Ser. 5, Vol 50-20 (1888)

[20] E.P. Vrahopoulou, A.J. McHugh; Shear-Thickening and structure formation in polymer solutions; Journal of Non-Newtonian Fluid Mechanics, 25, 157-175 (1987)

[21] J.G. Oldroyd; A rotational formulation of the equation of plastic flow for a Bingham solid; Mathematical Proceedings of the Cambridge Philiosophical Society; Vol 43, 100-105 (1947)

[22] J.Locat; Viscosity, yield stress, remodeled strength, and liquidity index relationships for sensitive clays; Canadian Geotechnical Journal; (1988)

[23] T. Hemphill, W. Campos, A. Pilehvari; Yield-power law model more accurately predicts mud rheology; Oil and Gas journal; Vol. 91-34 (1993)

[24] W.H. Bauer, E.A. Collins, in F.R. Eirich (Ed.), Rheology: Theory and Applications, Vol. 4, Academic Press, New York, (1967)

[25] J. Mewis; Thixotropy – a general review; Journal of non-Newtonian Fluid Mechanics, 6, Vol.1-20, (1979)

[26] Selected Definitions, terminology and Symbols for Rheological Properties, IUPAC, Oxford (2002)

[27] H. Freundlich; Thixotropy, influenced by the orientation of anisometric particles in sols and suspensions; Trans. Faraday Soc., (1935)

[28] L. V. Woodstock; Origins of thixotropy; Physical review Letters, Vol. 54-14, (1985)

[29] B.S. Chawla; Thixotropy and rheopexy of propyliodone suspensions in arachis oil: Effect of median particle size; Journal of Pharmacy and Pharmacology, Vol.20, 168-175, (1968)

[30] H. Freundlich; Some recent works on gels; Journal of Physical Chemistry; Vol. 41-7, 901-910, (1937)

[31] Maxwell Model of Viscoelasticity; Rheology of thixotropic coatings by Janes Vlrc.

[32] F.N. Cogswell; Converging flow of polymer melts in extrusion dies; Polym. Eng. Sci; 12, 64–73, (1972)

[33] Petrie J.S.; Extensional viscosity: A critical discussion; Journal of non-Newtonian Fluid Mechanics, Vol.137, 15-23, (2006)

[34] T.T. Dao, A.X. Ye, A.A. Shaito, N. Roye, K. Hedman; Capillary Rheometry: Analysis of Low-viscosity fluids and viscous liquids and melts at high shear rates; Reologica Instruments, American Laboratory; Technical Article, (2009)

[35] Hilton D.K., Van Sciver, S.W.; Absolute dynamic viscosity measurements of subcooled liquid oxygen from 0.15 MPa to 1.0 Mpa; Cryogenics, Vol.48, 56-60, (2008)

[36] Capillary Viscometer; Advanced Plastics and Testing Technologies CR-6000; Qualitest International Inc. 2009-2012

[37] Capillary Viscometer; Advanced Plastics and Testing Technologies CR-6000; Qualitest International Inc. 2009-2012 [http://www.worldoftest.com/capillary.htm]

[38] National Physical Laboratory, Guidelines on using a Rotational Viscometer; (2010) http://www.npl.co.uk/

[39] Schwarzl F.R.; Numerical calculations of storage and loss modulus from stress relaxation data for linear viscoelastic materials, Chemistry and Materials, Rheologica Acta, Vol.10, 165-173, (1971)

[40] Cone-Plate measuring system for a Rotational Rheometer; Pressure Profile Systems inc.; Rheological Applications; profile measurement systems; [http://www.dactyl.com/scratchpad/pps/rheology.html]

[41] P. Azerad, E. Baensch; Quasi-stability of the primary flow in a cone and plate viscometer; J. math. Fluid. Mech; 6, 253-271, (2004)

[42] D. B. Cox; Radial flow in the cone-plate viscometer; Nature 193, 670, (1962)

[43] M.E. Fewell, J.D. Hellmus; The secondary flow of Newtonian fluids in cone-and-plate viscometers; Trans. Soc. Rheol., Vol. 21, 535-565, (1977)

[44] Malvern Inc; Rheological Analysis Of Dispersions By Frequency Sweep Testing Using Equipment From Malvern Instruments, (2006)

[45] Franklin A.G., Krizek R.J.; Complex viscosity of a Kaolin clay; Clays and Minerals, Vol.17, 101-110, (1969)

[46] Shenoy A.V.; Rheology of Filled Polymer Systems; Springer, 1st Edition, (1999)

[47] C. Poisson, V. Hervais, M.F. Lacrampe, P. Krawczak; Optimization of PE/binder/PA extrusion blow-molded films. II. Adhesion properties improvement using binder/EVA blends; Journal of applied polymer science, Vol. 101, 118-127, (2006)

[48] F. Awaja, M. Gilbert, G. Kelly, B. Fox, P.J. Pigram; Adhesion of polymers; Progress in Polymer Science; Vol. 34, 948-968, (2009)

[49] W.C. Wake; Adhesion and the formulation of adhesives. 2nd ed.; Essex: Applied Science Publishers Ltd.; (1982)

[50] Myers D. Surfaces, interfaces, and colloids: principles and applications, 1st ed.; Weinheim: Willey VCH; (1991)

[51] A.J. Kinloch; The science of adhesion; Journal of Materials Science; Springer, 2141-2166, (1980)

[52] K.W. Allen; Some reflections on contemporary views of theories of adhesion; International Journal of adhesion and adhesives; Vol. 13, 67-72, (1993)

[53] H.R. Brown; Polymer Adhesion; Materials Forum Australia, Vol. 24, 49-58, (2000)

[54] D.E. Packham, K.L. Mittal; Adhesion Aspects of polymeric coatings; Proc. Symp., 1, Plenum Press, New York, NY (1983)

[55] E. Anancharoengwong; Synthesis and characterization of cis-1,4-polyisoprene based polyurethane coatings; study of their adhesive properties on metal surfaces; Chimie et Physicochimie des Polymers, Universite du Maine, Thesis, (2011)

[56] R.P. Wool; Adhesive Science and Engineering 2: Surfaces, Chemistry and Applications; Elsevier, chap. 8, 351, (2002)

[57] S.S. Voyutskii, V.L. Vakula; The role of diffusion phenomena in polymer-to-polymer adhesion; Journal of applied polymer science, Vol. 7, 475-491, (1963)

[58] K.W. Allen; A review of contemporary views of Theories of adhesion; Journal of Adhesion; Vol. 21, (1987)

[59] L.H. Sharpe; The Interfacial Interactions in Polymeric Composites, 230, (1993)

[60] A.J. Kinloch; Adhesion and Adhesives: Sciences and Technology, Journal of Mathematical Sciences, Vol. 15, 66, (1980)

[61] M. Matsuda, H. Komada; Direct bonding between poly(oxy-2,6-dimethyl-1,4-phenylene) and rubber with radicals; Vol. 95, 53-59, (2005)

[62] R. Bailey, J.E. Castle; XPS study of the adsorption of ethoxysilane on iron; Journal of Material Science, Vol. 12-10, 2049-2055, (1977)

[63] M. Gettings, A.J. Kinloch; Surface analysis of polysiloxane/metal oxide interfaces; Journal of Material Science, Vol. 12-12, 2511-2518, (1977)

[64] V.E. Basin; Advances in understanding the adhesion between solid substartes and organic coatings; Progress in organic coatings, Vol. 12, 213-250, (1984)

[65] M.A Chen, H.Z. Li, X.M. Zhang. International Journal of adhesion and adhesives; Vol. 27-3, 87, (2007)

[66] S.S. Voyutskii. Auto adhesion and adhesion of high polymers; Willey Interscience Publishers; (1963)

[67] Y.S. Lipatov; Polymer reinforcement; ChemTech Publishings, (1995)

[68] Feinerman A.E., Lipatov Y.S., Minkov V.I.; Interfacial Interactions in Polymers: The Dependence of the Measured Surface Tension of Solid Polymer on the Surface Tension of Wetting Liquid; The Journal of Adhesion, Vol.61, 37-54, (1997)

[69] T. Reintjes (editor); Solubility enhancement with BASF Pharma polymers; Solubilizer Compendium, BASF Pharma GmbH, (2008)

[70] Calcium Stearate; Executive summary for processing by the USDA Organic national Program from UC SAREP; (2002)

[71] Chemical Stucture of SoluPlus, taken from Solubility enhancement with BASF Pharma polymers; Solubilizer Compendium, BASF Pharma GmbH, (2008)

[72] Anton Paar Ind. Rheometer MCR301 taken from http://www.anton-paar.com/

[73] Roblegg E., Jaeger E., Hodzic A., Koscher G., Mohr S., Zimmer A., Khinast J.; Development of sustained release lipophilic calcium stearate pellets via hot melt extrusion; European journal of pharmaceutics and Biopharmaceutic, Vol.79, 635-645, (2011)

[74] A. Zosel; The effect of fibrillation on the tack of pressure sensitive adhesives; Int. J. of Adhesion &Adhesives, Vol.18, 265-271, (1998)

Appendix

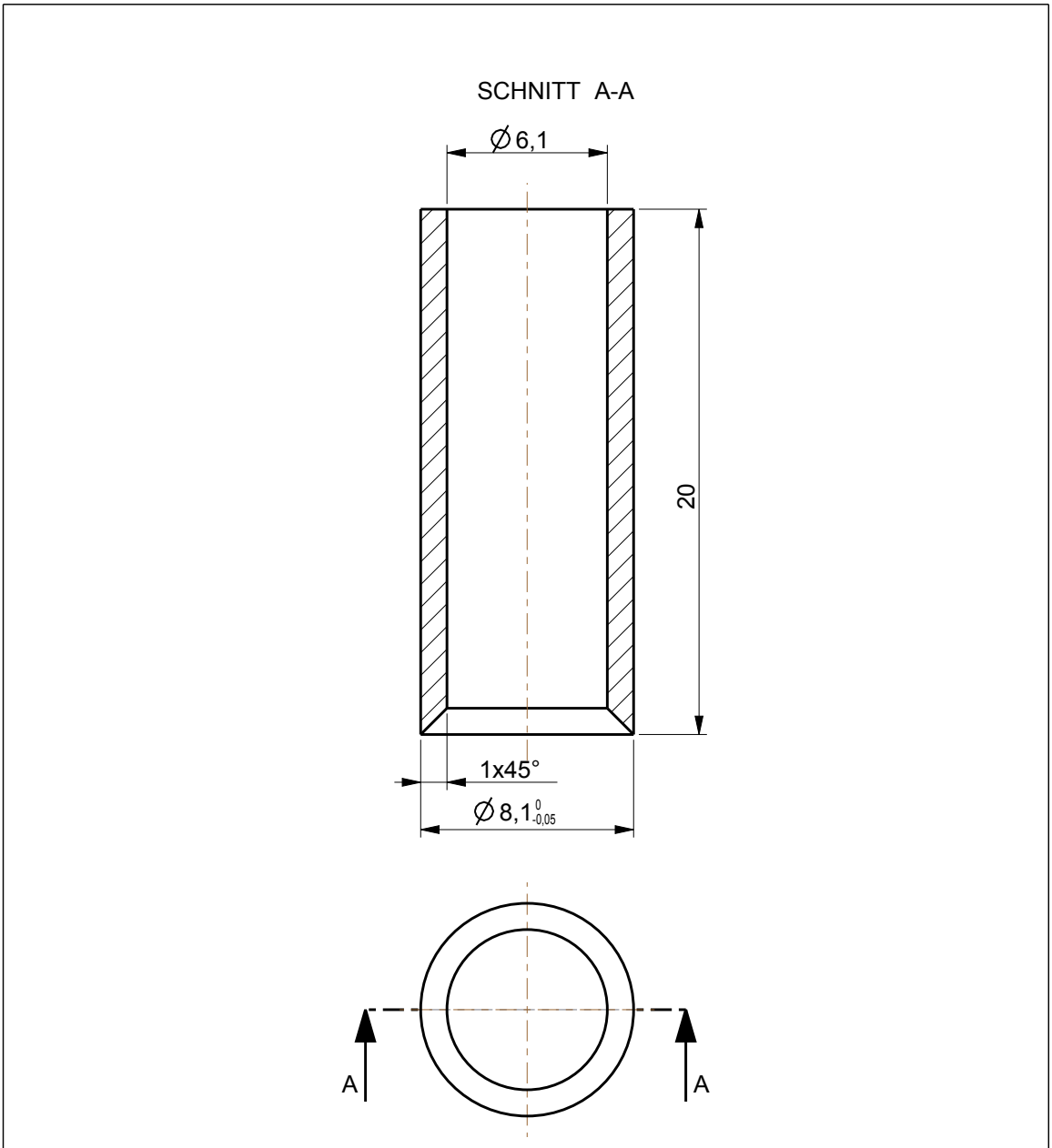

Verwendungsbereich				Oberflaeche			Masstab 5,000	Gewicht
				Allgemeintoleranz ISO 2768-mK			Werkstoff/Halbzeug	
					Datum	Name	Benennung	
				Bearb.	20.07.2012	D. Treffer	Rohr 8 mm	
				Gepr.				
				Norm				
				Komm.-Nr.:				
				RCPE GmbH			Zeichnung/Sach-Nr.:	Blatt 1
Zust.	Aenderung	Datum	Name					Bl.
							Ers.f.:	Ers.d.:

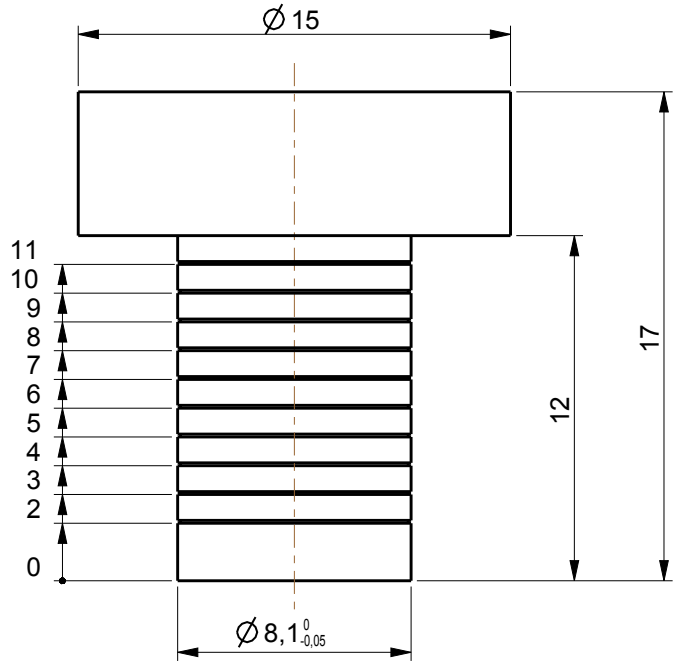

Verwendungsbereich				Oberflaeche	Masstab 5,000	Gewicht
				Allgemeintoleranz ISO 2768-mK	Werkstoff/Halbzeug	
				Datum / Name	Benennung	
				Bearb. 20.07.2012 D. Treffer	Stempel 8 mm	
				Gepr.		
				Norm		
				Komm.-Nr.:		
				RCPE GmbH	Zeichnung/Sach-Nr.:	Blatt 1 / Bl.
Zust.	Aenderung	Datum	Name		Ers.f.:	Ers.d.:

SCHNITT A-A

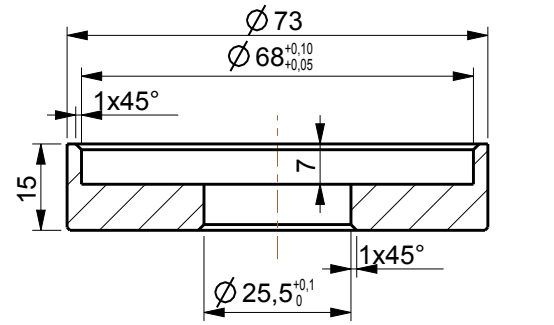

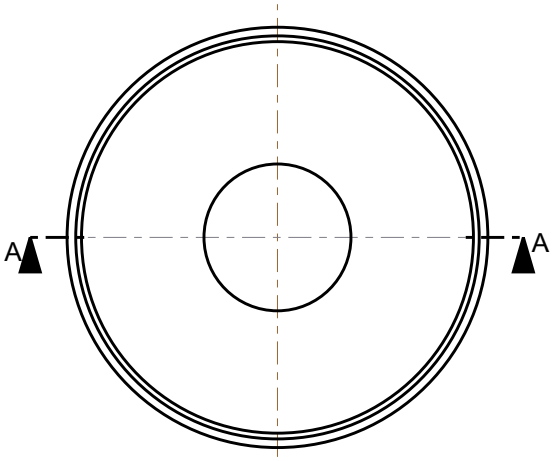

Verwendungsbereich				Oberflaeche		Masstab 1,000 / Gewicht
				Allgemeintoleranz ISO 2768-mK		Werkstoff/Halbzeug
					Datum	Name
				Bearb.	20.07.2012	D. Treffer
				Gepr.		
				Norm		
				Komm.-Nr.:		Benennung: Zentrierring
				RCPE GmbH		Zeichnung/Sach-Nr.: / Blatt 1 / Bl.
Zust.	Aenderung	Datum	Name			Ers.f.: / Ers.d.:

SCHNITT A-A

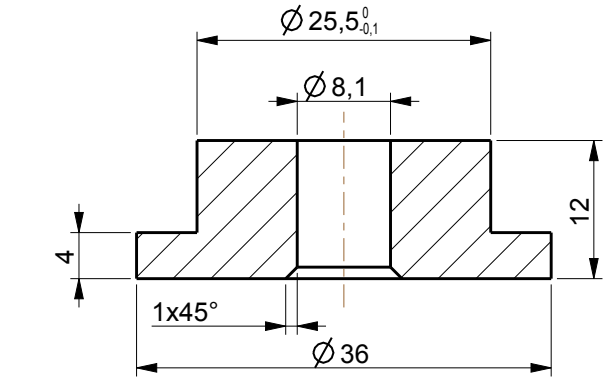

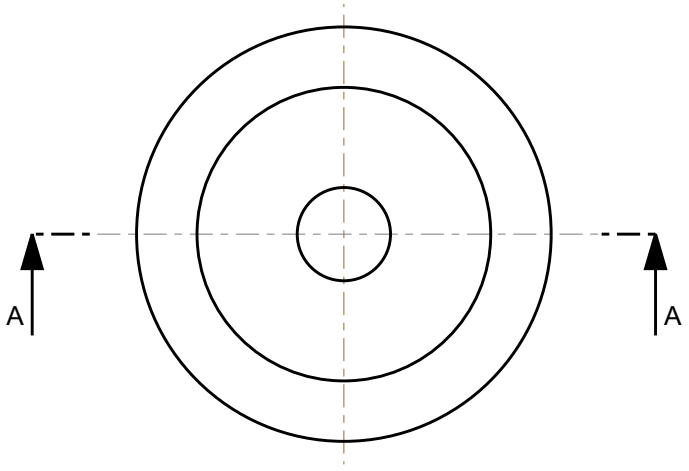

Verwendungsbereich				Oberflaeche			Masstab 2,000		Gewicht
				Allgemeintoleranz ISO 2768-mK			Werkstoff/Halbzeug		
					Datum	Name	Benennung		
				Bearb.	20.07.2012	D. Treffer	Einsatz 8 mm		
				Gepr.					
				Norm					
				Komm.-Nr.:					
				RCPE GmbH			Zeichnung/Sach-Nr.:		Blatt 1
									Bl.
Zust.	Aenderung	Datum	Name				Ers.f.:	Ers.d.:	